esa

ECOSPHERE

An indicator-based decision framework for the northern California red abalone fishery

William J. Harford,[1,†] Natalie A. Dowling,[2] Jeremy D. Prince,[3] Frank Hurd,[4] Lyall Bellquist,[4] Jack Likins,[5] and Jono R. Wilson[4,6]

[1]*Cooperative Institute of Marine and Atmospheric Studies, Rosenstiel School of Marine and Atmospheric Studies, University of Miami, Miami, Florida 33149 USA*
[2]*CSIRO Oceans and Atmosphere, G.P.O. Box 1538, Hobart, Tasmania 5001 Australia*
[3]*Biospherics Pty Ltd, P.O. Box 168, South Fremantle, Western Australia 6162 Australia*
[4]*The Nature Conservancy, 555 Capitol Mall, Suite 1195, Sacramento, California 95814 USA*
[5]*Gualala, California, USA*
[6]*Bren School of Environmental Science & Management, UCSB, Santa Barbara, California 93106 USA*

Citation: Harford, W. J., N. A. Dowling, J. D. Prince, F. Hurd, L. Bellquist, J. Likins, and J. R. Wilson. 2019. An indicator-based decision framework for the northern California red abalone fishery. Ecosphere 10(1):e02533. 10.1002/ecs2.2533 [Correction: article updated on January 8, 2019, after initial online publication: The year of publication in the suggested citation for this article was changed from 2018 to 2019.]

Abstract. Among abalone species that were once harvested along the California coastline, red abalone (*Haliotis rufescens*) supports the remaining recreational fishery. To support development of a red abalone fishery management plan, non-governmental organizations have initiated expanded data collection and developed fishery management strategies. The latter is the subject of this study, as we present a management strategy evaluation (MSE) of a multi-indicator decision tree. The decision tree relies on landings from each of 56 fishing sites and length frequency information collected during fishery-independent diver surveys at a subset of sites. The decision tree was designed to cope with existing data limitations and to ensure that localized meta-population dynamics were adequately considered in decision-making. It was also necessary to balance the potential for localized abundance changes with the practical issue of implementing fishery regulations at larger spatial scales. The MSE demonstrated that undesirably low stock sizes could be avoided while also continuing to maintain a viable fishery, even under environmental conditions that are detrimental to abalone populations. Under less-severe environmental conditions, stock size was maintained, on average, above the biomass associated with production of maximum sustainable yield. Our discussion centers on steps that were taken to refine the decision tree and to incorporate feedback from scientists and stakeholders and to facilitate transparent evaluation of management options.

Key words: abalone; data-limited; data-poor; ecosystem-based fishery management; *Haliotis rufescens;* harvest strategy; invertebrate fishery; management procedure; management strategy evaluation (MSE); spatial model.

Received 17 April 2018; revised 1 November 2018; accepted 6 November 2018. Corresponding Editor: Hunter S. Lenihan.

† **E-mail:** wharford@miami.edu

Introduction

Data-limited fisheries management typically proceeds in the absence of quantitative stock assessment, relying instead on simpler indicators derived from monitoring data to inform decision-making. Circumstances contributing to data limitations are varied but can arise for example where fine-scale spatial stock structure is at odds with feasible scales of data collection or where an overwhelming number of fishers and landing sites prevents comprehensive

monitoring (Prince et al. 2008, Butterworth et al. 2010, Dowling et al. 2015*a*). These types of data limitations are facing management of the California recreational fishery for red abalone (*Haliotis rufescens*). Fishing occurs along the northern California coast between San Francisco and the Oregon border, and is estimated to be worth at least US$24 million and involves approximately 31,000 registered fishers (Reid et al. 2016). In addition, historical collapses of other abalone stocks have spurred interest in ensuring sustainability of this remaining fishery (Erlandson et al. 2005, Braje 2016).

The red abalone fishery is regulated under the State of California Department of Fish and Wildlife (CDFW) Abalone Recovery and Management Plan (CDFW 2005). But recently, a research diver-based survey of red abalone density, which is heavily relied upon for regulatory decision-making, was the subject of scientific review. Convened by California's Ocean Science Trust (OST), this review recommended fundamental improvements to biological assessment of red abalone (OST 2014). The CDFW has subsequently initiated development of a red abalone fishery management plan. In support of this initiative, non-governmental organizations have engaged with recreational fishers to expand data collection and to develop candidate management strategies. A protocol for cost-effective monitoring of red abalone length composition has been successfully implemented by the citizen scientist group Reef Check California (Freiwald et al. 2016). In connection with advancements in resource monitoring, The Nature Conservancy has collaborated with independent fisheries scientists to develop and evaluate data-limited management strategies for the red abalone fishery. Management strategy development was motivated by similar approaches utilized by Australian abalone fisheries (Prince et al. 2008).

Here, we report on evaluation of candidate management strategies that were designed to overcome several issues facing the California red abalone fishery. Developing management strategies for the red abalone fishery is complicated by the prevalence of localized (e.g., sites <1000 m apart) spatial differences in abalone species growth, survival, and reproductive success (Emmett and Jamieson 1988, Sloan and Breen 1988, Nash 1992, Haaker et al. 1995, McShane and Naylor 1995, Leaf et al. 2007, Geibel et al. 2010). Globally, it is well established that the small-scale meta-population dynamics of abalone species need to be accommodated in management strategies (Shepherd and Brown 1993, Prince 2005, Saunders et al. 2008, Mayfield et al. 2012, Bedford et al. 2013). Problematically, within the California red abalone fishery, <50% of fishing sites along the coastline are monitored, aside from recording of catches, and sites may differ with respect to fishing pressure, oceanographic conditions, and habitat availability. Thus, in relying on existing data streams, candidate management strategies need to accommodate site-specific signals about resource changes where this information is available, while also guiding regulatory adjustments along the entire coast (Fig. 1). Because the northern California coastline consists of approximately 56 fishing sites, a pragmatic balance was also desirable between deploying fine-scale resource monitoring and implementing regulatory tactics at a larger regional spatial scale. Regional regulatory tactics are a practical necessity for both fishers

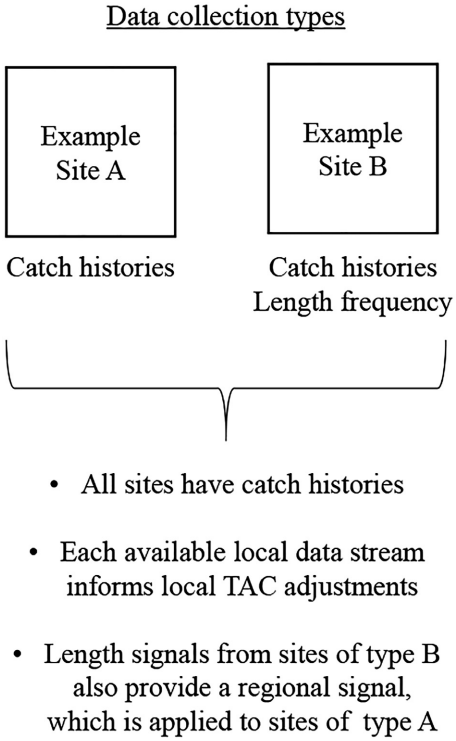

Fig. 1. Data availability and its influence on harvest control rule design.

and fishery enforcement. Currently, tactical regulation of red abalone catches includes a ban on scuba, a minimum shell length of 178 mm (7 inch) for possession, seasonal and area closures, and daily and annual bag limits that vary by management region. In addition, CDFW closed the red abalone fishery for the 2018 season, citing ecological and environmental conditions that have been detrimental to red abalone abundance, and thus, stock rebuilding considerations also entered into our considerations for management strategy design.

Given the spatial complexity of the red abalone fishery, management strategy design could not be adequately addressed through expert judgment alone. Accordingly, management strategies were subjected to simulation testing using management strategy evaluation (MSE; Butterworth and Punt 1999, Smith et al. 1999, Sainsbury et al. 2000, Butterworth 2007, Punt et al. 2016). MSE examines the collective performance of data collection, data analysis, and decision-making in terms of whether fishery objectives are expected to be achieved over various time horizons. The effects of uncertainty on decision-making are also explicitly addressed in MSE, for instance, by replicating the error structure or bias of a monitoring program and propagating this (potentially unreliable) information into application of an HCR. MSE is also well suited to examining management reactions to environmental changes that may affect stock status because MSE simulates recursive decision-making through time, where each decision is supplied with updated information, and thus, each decision is a reaction to a new set of conditions (A'mar et al. 2010, Punt et al. 2014).

In this study, we used MSE to evaluate candidate management strategies for the red abalone fishery. In conducting MSE, we first measured the expected performance of management strategies under simulation scenarios reflecting uncertainty about the future severity of environmental conditions. We then evaluated considerations related to stock recovery in the context of the trade-off between reduction of catches and the expected pace of stock recovery. Finally, the open-access nature of this recreational fishery motivated us to consider how our decision tree framework could accommodate regulatory tactics, like annual bag limits, which are more practical for recreational fisheries than TACs. Collectively, our MSE contributes guidance to specification of several central constituents of the red abalone fishery management plan.

Methods

Preliminary development of management strategies and stakeholder feedback

Through MSE and through feedback from stakeholders and scientists with interest in the red abalone fishery, our initial phase of management strategy development highlighted the need for a variety of refinements (Harford et al. 2017). Initially, management strategies were formulated as multi-indicator frameworks that relied on fishery-independent density surveys, catch histories, length frequency distributions, and a climate index. These indicators collectively contributed to an HCR that was hierarchically structured as a decision tree. Like other data-limited harvest strategies that rely on small incremental regulatory changes through time, our decision tree determined the direction of total allowable catch (TAC) adjustments and iteratively modified TACs in small steps until catches stabilized around target reference points.

Refinements to the MSE consisted of proceeding without density surveys given concerns about data reliability (OST 2014). We also excluded a climate index, namely an index of anomalies of the El Nino Southern Oscillation. This index was proposed to reflect shifts between desirable and undesirable environmental conditions, recognizing that red abalone growth and survival can vary dramatically in response to climate variation and its effects on kelp biomass (e.g., *Nereocystis luetkeana*), which is red abalone's main dietary constituent (Tegner and Dayton 1987, Tegner et al. 2001, Jiao et al. 2010, Cavanaugh et al. 2011, Rogers-Bennett et al. 2011). However, this climate index was subsequently excluded because, in reality, mechanistic linkages between red abalone biology and environmental conditions are typically difficult to confirm and because environmental indices typically fail to improve management performance unless mechanistic relationships are well established (A'mar et al. 2010, Punt et al. 2014). Based on our initial analyses, site-specific catch histories and length frequency distributions offered the most potential as useful inputs to HCRs for the red abalone fishery, given that our management strategy

designs were constrained to existing data streams. Length frequency distributions were used to calculate spawning potential ratio (SPR), which is a measure of the state of reproductive potential of the stock and a proxy for spawning stock density (Goodyear 1993, Shepherd and Baker 1998, Hordyk et al. 2015*c*). Catch histories were used in a Monte Carlo method, known as catch-MSY, to estimate site-specific harvest rates relative to a harvest rate reference point (Martell and Froese 2012, Froese et al. 2017).

Operating model

Spatial distribution of red abalone.—Stock dynamics were a spatially explicit representation of red abalone inhabiting the northern California coastline. Abalone were distributed along a one-dimensional array consisting of 56 sites, each of which corresponded to a recreational fishing location that spans a total distance of approximately 540 km (334 miles) from San Francisco to the California–Oregon border (Tables 1 and 2). Given that each site corresponded to an area of one to tens of kilometers, we did not model site connectivity because larval dispersal and adult movement likely occur on much smaller spatial scales. Short larval durations of abalone species typically act to minimize dispersal distances from 10s to 100s of meters (Prince et al. 1987, McShane et al. 1988, Shepherd and Brown 1993, Leighton 2000). While potential for long-distance larval dispersal has been suggested (Watson et al. 2010, Rogers-Bennett et al. 2016), most evidence demonstrates that nearly all new recruits come from parents located within several hundred meters (Gruenthal et al. 2007, Temby et al. 2007, Saunders et al. 2008). Adult movement over various timescales is also thought to be limited to 100s of meters (Ault and Demartini 1987, Coates et al. 2013). In addition, we did not explicitly represent separation between deep-water habitat that is inaccessible to free-diving fishers and shallow-water areas where fishing occurs because the scale of adult movement is likely to connect populations across these habitats. The operating model and evaluation of management strategies, in their entirety, were implemented in the R statistical computing environment (R Development Core Team 2012).

Temporal dynamics of red abalone.—Temporal dynamics were formulated using length-structured population dynamics, which is an approach well suited for modeling species that are difficult to age, like marine invertebrates (Breen et al. 2003, Haddon 2011). Length-based models account for survival, growth, and reproduction through time by assigning individuals to length classes or length bins. Numbers-at-length matrices differ from numbers-at-age matrices because the latter tracks specific cohorts as they transition between age classes, while the former probabilistically tracks transitions between length classes where individuals from several cohorts are likely to be found in any given length bin (Haddon 2011). The red abalone stock was initialized for the year 2002, and historical temporal dynamics were modeled for the time period of 2002–2016, using actual site-specific catches, before generating 25 yr forward forecasts during which time candidate management strategies were implemented and used to modify fishery regulations.

Numbers of red abalone were assigned to length classes from 5 mm to 320 mm, with bin sizes increasing in 5 mm increments. For a given site l and simulation replicate k, the matrix algebra involved in calculating the progression of individuals between length bins, according to an annual time step, j, was (for brevity, k and l subscripts are omitted):

$$\mathbf{N_{j+1}} = \boldsymbol{G}_j(\boldsymbol{S}_j\mathbf{N_j}) + \mathbf{R_j}, \quad (1)$$

where $\mathbf{N}$ is the abundance vector of length classes, $\boldsymbol{G}$ is the square growth transition matrix with upper triangle of zeros preventing negative growth in length, $\boldsymbol{S}$ is a diagonal matrix representing survival at length, and $\mathbf{R}$ is the recruitment vector. The growth matrix specified how numbers-at-length would transition probabilistically into other length classes based on a Gaussian probability density function with expected growth increments obtained from a von Bertalanffy function (i.e., expected growth increment is $\Delta L_{i,j,k,l} = (L\infty_{j,k,l} - L_{\text{bin},i})(1 - \exp(-K_{k,l}))$, where K is Brody growth coefficient, $L\infty$ is average maximum size, and L_{bin} is the lower bound of each length bin, i) and standard deviation of 8.5 mm (Rogers-Bennett et al. 2007). The subscript j indicates parameters that were time-varying. In the subsequent section (*Methods: Operating model: Environmentally driven life history variation*), we describe our approach for generating environmentally driven spatial and temporal variation in life history parameters.

Table 1. Summary of sites in Del Norte, Humboldt, and Mendocino counties.

Site	Region	Mean catch 2002–2016	Catch 2016	Not take zone	Reef check sampling	CDFW sampling
Crescent City	1	135	79			
Other Del Norte	1	45	6			
Patrick's Point	1	585	343			
Trinidad	1	326	198			
Punta Gorda	1	788	182			
Shelter Cove	1	3041	1557			
Other Humboldt	1	619	209			
Bear Harbor	1	386	282			
Usal	1	239	77			
Hardy Creek	1	1373	669			
Abalone Point	1	2871	1445			
Westport	1	1805	974			
Bruhel Point	1	645	188			
Kibesillah	1	572	0	Yes		
MacKerricher	1	4690	3204			
Glass Beach	1	5475	5685		Yes	
Georgia Pacific	1	7316	5627			
Todds Point	1	7259	6272			Yes
Hare Creek	1	4605	2949			
Mitchell Creek	1	2685	2290			
Jughandle	1	5714	6464			
Caspar Cove	1	6597	6283		Yes	Yes
Russian Gulch	1	7097	8110		Yes	Yes
Jack Peters Gulch	1	3792	8404			
Mendocino Hdlnds	1	10,371	12,222		Yes	
Gordon Lane	1	3140	4424			
Van Damme	1	16,525	17,051		Yes	Yes
Dark Gulch	1	4636	5941			
Albion Cove	1	7688	6016			
Salmon Creek	1	1654	1449			
Navarro River	1	3306	2447			
Elk	1	8193	6506			
Point Arena Lighthouse	1	4387	1010		Yes	
Arena Cove	1	8993	4040		Yes	Yes
Moat Creek	1	9592	5132			
Schooner Gulch	1	539	161			
Saunders Landing	1	701	0	Yes		
Anchor Bay	1	4965	3785			
Robinson Point	1	1327	1414			

Note: Catches are in numbers of abalone; sampling coverage at the time of publication; CDFW is California Department of Fish and Wildlife.

Maturity schedules were time-invariant but did reflect site-specific growth differences. At each site, a logistic maturity function ($Mat_{i,k,l}$) was parameterized based on average maximum size ($\bar{L}\infty_{k,l}$) and the life history relationships: $L50_{k,l} = \bar{L}\infty_{k,l} \times 0.48$ and $L95_{k,l} = L50_{k,l} \times 1.15$, where $L50$ and $L95$ are the lengths associated with 50% and 95% probabilities of maturity, respectively. These relationships conform to established relationships that are known as Beverton-Holt life history invariants (Jensen 1996, Prince et al. 2015), but which have been modified to reflect available life history information for California red abalone. Appendix S1 describes how the ratios $L50/L\infty$ and $L95/L50$ were obtained from analysis of empirical growth and maturity patterns of red abalone from the northern California coastline, based on previous studies (Rogers-Bennett et al. 2004, 2007).

Table 2. Summary of sites in Sonoma and Marin counties.

Site	Region	Mean catch 2002–2016	Catch 2016	Not take zone	Reef check sampling	CDFW sampling
Gualala Point	2	850	321			
Sea Ranch	2	10,803	5723		Yes	Yes
Black Point	2	244	26			
Stewarts Point	2	1098	153			
Rocky Point	2	232	39			
Horseshoe Cove	2	1038	0	Yes		
Fisk_Mill Cove	2	5542	1415			
Salt_Point State Park	2	8555	4197		Yes	Yes
Ocean Cove	2	4293	2897		Yes	Yes
Stillwater Cove	2	3747	3147		Yes	
Timber Cove	2	7625	3681			Yes
Fort Ross	2	28,672	2366		Yes	Yes
Jenner	2	2515	963			
Bodega Head	2	902	263		Yes	
Tomales Point	2	1968	561			
Point Reyes	2	281	31			
Other Marin	2	424	124			

Note: Catches are in numbers of abalone; sampling coverage at the time of publication; CDFW is California Department of Fish and Wildlife.

Maturity-at-length was linked to emergence-at-length. This linkage reflects an ontogenetic shift from cryptic juveniles, hidden in crevices, to mature adults that inhabit exposed substrates (Prince et al. 1988). Using data collected from the fishing site known as Van Damme (see Rogers-Bennett et al. 2004), this linkage was established by comparing the $L50$ obtained from histological examination to the left-hand side of the observed length frequency distribution, which reflects emergence of red abalone. By aligning the cumulative probability of emergence-at-length with the histologically derived $L50$, we were able to identify the cumulative emergence probability associated with $L50$. For Van Damme, this quantity was 0.17. Thus, logistic emergence was specified to mirror the maturity curve, except that the emergence curve was shifted so it passed through the point ($L50$, 0.17). Modeling emergence was necessary to reproduce simulated length frequency sampling (of emergent red abalone) and to incorporate any effect of emergence on fishery selectivity. Additional details are in Appendix S1.

Eggs-per-female was an exponential function of length ($\text{fec}_i = \exp(-10.434)L_{\text{mids},i}^{4.701}$; L_{mids} is mid-point of each length bin), with parameter estimates obtained by fitting this exponential function to digitized length-fecundity data from Rogers-Bennett et al. (2004). Numbers of recruits at each site were calculated according to the Beverton-Holt stock–recruitment function that was re-parameterized using steepness (h):

$$R_{j,k,l} = \left(\frac{0.8R_{0,k,l}hB_{j-1,k,l}}{0.2B_{0,k,l}(1-h)+(h-0.2)B_{j-1,k,l}}\right) \exp\left(d_{j,k,l}-\sigma^2/2\right), \quad (2)$$

where d is a recruitment deviation for each combination of year, site, and simulation replicate, which is specified to have a normal distribution with mean zero and with standard deviation σ. B_0 is unfished egg production, and B is a measure of reproductive output summed across length bins, i, in year $j-1$:

$$B_{j-1,k,l} = \sum_i \text{Mat}_{i,k,l} \times \text{fec}_i \times \text{N}_{i,j-1,k,l} \quad (3)$$

Steepness was specified as 0.6, as abalone species tend to display weak compensatory recruitment at low stock size and this value is similar to those assumed in abalone stock assessments (Gorfine et al. 2005, Zhang et al. 2007, Rossetto et al. 2013, Fu 2014). The Allee effect has been suggested as being an important limitation to reproduction at low density, although exact reproductive thresholds are difficult to identify (Tegner et al. 1989, Shepherd and Brown 1993,

Catton et al. 2016). In our stock–recruitment simulations, we forced complete recruitment failure to occur when reproductive output fell below 1% of unfished reproductive output. Biomass fell below this threshold in 13% of forecast across year–site combinations during our simulations of severe environmental conditions and low historical red abalone depletion levels (see *Methods: Baseline performance testing*). This assumption was later examined in sensitivity runs that are reported in Appendix S3. Age 1 recruits ($R_{i,j}$) populated length bins of the recruitment matrix ($\mathbf{R}_j$) according to a Gaussian probability density function with expected length calculated according to site-specific average von Bertalanffy parameters ($\bar{L}\infty_{k,l}$ and $\bar{K}_{k,l}$) and standard deviation in length-at-age one of 8.5 mm (Rogers-Bennett et al. 2007).

Survival (S) consisted of natural mortality (M) and fishing mortality (F) and was calculated at the beginning of each time step:

$$S_{i,j,k,l} = \exp\left(-M_{i,j,k,l} - \text{sel}_{i,j}F_{j,k,l}\right), \quad (4)$$

where sel is selectivity and is a function of red abalone emergence and specified minimum possession size. For a given l and k, $S_{i,j}$ populates the diagonal of the corresponding survival matrix ($\mathbf{S}_j$). Average natural mortality-at-length was obtained from Leaf et al. (2008) who describe natural mortality as being 0.65 yr^{-1} for shell lengths less than 50 mm, 0.05 yr^{-1} for length >245 mm, and a decreasing logistic function in between. Catch in numbers (C^{N}) is calculated:

$$C^{\text{N}}_{i,j,k,l} = \frac{\text{sel}_{i,j}F_{j,k,l}}{(M_{i,j,k,l} + \text{sel}_{i,j}F_{j,k,l})}(1 - S_{i,j,k,l})\text{N}_{i,j,k,l}, \quad (5)$$

And catches in weight (C^B; kg) is:

$$C^B_{i,j,k,l} = C^{\text{N}}_{i,j,k,l}W_i \quad (6)$$

Environmentally driven life history variation.— Spatial variation was simulated by generating site-specific mean asymptotic length ($\bar{L}\infty_{k,l}$) and Brody growth coefficient ($\bar{K}_{k,l}$) according to a multivariate Gaussian distribution (MVN(μ, Σ)) with $\mu = (\bar{L}\infty = 254, \bar{K} = 0.108)$ and using a standard deviation of 8.5 on $\bar{L}\infty$, 0.006 on $\bar{K}$, and a correlation coefficient of 0.6 to obtain the variance–covariance matrix, Σ (Rogers-Bennett et al. 2007, Geibel et al. 2010). Maturity- and emergence-at-length functions were parameterized based on site-specific mean growth parameters, thus enabling growth and reproductive characteristics to co-vary at each site (Prince et al. 2015).

The life history parameters $L\infty$ and natural mortality were time-varying and were correlated with an index of the El Nino Southern Oscillation (ENSO) known as the Ocean Nino Index, which measures surface temperature anomalies (NOAA 2017). This index was not considered to be an exhaustive environmental driver of red abalone dynamics, but we did consider this index to have reasonable statistical properties of prevailing climate fluctuations. Through laboratory experiment, water temperature has been shown to negatively affect red abalone gamete production, body condition, survival rates, and somatic growth (Vilchis et al. 2005, Perez 2010, Moore et al. 2011). In an observational study, Jiao et al. (2010) reported a negative correlation between $L\infty$ and warm-phase temperature anomalies of the El Nino Southern Oscillation Index. Likewise, trends in food availability, especially related to climate- and storm-induced variability in kelp biomass (e.g., *Nereocystis luetkeana*), have been implicated in changes to red abalone survival and growth (Tegner and Dayton 1987, Tegner et al. 2001, Cavanaugh et al. 2011, Rogers-Bennett et al. 2011). During the time period of 2002 to 2016, actual ENSO autumn season means (i.e., the September through November average) were used in constructing historical stock dynamics. To produce forecasts, we randomly selected toroidal-like segments of the autumn season ENSO index from the time period of 1950–2016 in an effort to preserve temporal autocorrelation.

Given generation of an ENSO index, time series of $L\infty$ and natural mortality were generated using a Cholesky transformation. We opted to link $L\infty_{j,k,l}$ with the ENSO index using a negative correlation of 0.5 and $L\infty_{j,k,l}$ varied in magnitude based on a Gaussian CV of 0.05 around the corresponding parameter $\bar{L}\infty_{k,l}$ (Jiao et al. 2010). Correlation strength reflected observational studies that have demonstrated statistically significant correlations between climate signals and red abalone growth parameters (Jiao et al. 2010) or kelp biomass (Cavanaugh et al. 2011), albeit reported correlation strengths varied considerably among studies. To link natural mortality with the ENSO index, we specified a positive correlation of 0.5

and modeled this linkage to be Gaussian on a log scale. The lognormal variance was specified such that at the most extreme positive ENSO anomaly, M-at-length reflected a 40% reduction in survival (i.e., survival = $\exp(-M)$), and at the most extreme negative ENSO anomaly, a corresponding increasing in survival occurred. Magnitudes of changes in natural mortality reflected experimental comparisons of red abalone survival between ambient conditions and those representing a severe El Nino warm event, which produced between 20% and 60% decreases in adult survival (Vilchis et al. 2005, Moore et al. 2011). Having both $L\infty$ and natural mortality co-vary with ENSO anomalies produced demographic changes that were more systematic in response to environmental conditions than would occur if life history parameters varied independently from one another. In addition, we found that previous studies were generally informative about variance in temporal fluctuations of life history parameters but were less informative about linkages to sources influencing this variation (Leaf et al. 2007, Geibel et al. 2010, Jiao et al. 2010). Thus, in constructing these relationships with the ENSO index we conserved the total variance of life history parameters, while assigning directional influence to a climate driver that reasonably reflected prevailing environmental conditions.

Recruitment deviations were lognormal with a standard deviation of 0.2. Deviations were independent of other environmental signals. We also simulated recruitment failures (generated independently for each site and simulation run) to reflect studies that have reported apparent absences of red abalone recruitment (Tegner et al. 1989, Karpov et al. 1998, Rogers-Bennett et al. 2016). These events were generated as a Bernoulli random variable with recruitment failure probability of 0.25, or thus, occurring on average once per every four years.

Time-varying natural mortality increases caused by non-anthropogenic sources, like harmful algal blooms or starvation, were generated as regional signals (separate signals for each of two regions) affecting either the northern fishing sites (Mendocino, Humboldt, and Del Norte counties) or the southern fishing sites (Sonoma and Marin counties). This approach accommodated observations both about the formation of localized algal blooms and about the large-scale oceanographic conditions that initiate these events (Trainer et al. 2000, Anderson et al. 2008, Rogers-Bennett et al. 2012). A lognormal distribution representing the relative strength of harmful algal blooms was constructed based on the approximated severity of the 2011 event (Rogers-Bennett et al. 2012). It is suspected that the 2011 event may have caused a threefold increase in natural mortality relative to the average adult natural mortality rate. Our simulated sampling distribution had a lognormal mean of one, and the occurrence of a threefold natural mortality multiplier occurred at the 97.5th percentile. Thus, our approach recognizes the threefold increase in natural mortality to be the previously estimated maximum recorded event strength, while also recognizing the possibility that more severe events could arise from sampling the tail of the lognormal distribution. Annual episodic events were multiplied against M-at-length for all lengths greater than the site-specific $L50$, reflecting non-anthropogenic changes in natural mortality dominantly affecting emergent red abalone. An exception to the probabilistic generation of red tide events was during 2011, where we imposed threefold multiplier to sites in Sonoma County and southward (in all simulation runs) to reflect reports of this severe event (Rogers-Bennett et al. 2012).

Simulated monitoring of red abalone.—In the operating model, observation of catches occurred without error. Observation of length frequency distributions was simulated at 15 sites that are routinely monitored by either CDFW or Reef Check California (Tables 1 and 2; CDFW 2005, Freiwald et al. 2016). Lengths were observed as a multinomial process with an effective sample size of 100 individuals, which is a reasonable sampling variance assumption for collection of length composition data (Hulson et al. 2012). Availability of length classes to the simulated survey was affected by site-specific emergence. Both Reef Check and CDFW do not annually sample all 15 sites. During the time period of 2002–2016, the actual schedule of sampling events was imposed on simulation runs. During the forecast time period, 9 of 13 sites monitored by Reef Check were randomly selected annually and 3 of 10 sites monitored by CDFW were likewise randomly selected to

reflect current sampling intensity. Site selection is not currently coordinated between these two organizations and was not coordinated in our simulations. In connecting simulated data to the indicator-based decision tree, we also implemented a three-year delay between data collection and its application to decision-making as a caution against institutional delays that may occur.

Indicator-based decision tree

The red abalone decision tree used catches (numbers of legal sized red abalone) and length frequency distributions to inform regulatory adjustments (Table 3). Catches at each site were used in conjunction with the catch-MSY approach to calculate the ratio of last year's harvest rate (U) to the harvest rate associated with production of MSY (maximum sustainable yield; Martell and Froese 2012). Length frequency data were used to calculate spawning potential ratio (SPR) using the LB-SPR library in R (Hordyk et al. 2015*a*, *b*, *c*, 2016). The SPR describes the reproductive potential of an exploited stock relative to its reproductive potential in an unexploited state (Goodyear 1993, Restrepo and Powers 1999). Regulatory adjustments refer to either setting annual TACs or modifying annual recreational bag limits. Our decision tree linked pre-specified regulatory adjustments to each combination of status indicators (Fig. 2). Magnitudes of regulatory adjustments, to TACs for instance, ranged between −20% and 20% from year to year based on observed quantities of status indicators. Decision tree design reflected the population biology of red abalone and past

Table 3. Rationale for the decision tree based on indicators of spawning potential ratio (SPR) and exploitation status calculated via catch-MSY approach.

SPR indicator	Catch-MSY indicator	Exploitation status	TAC adjustment (%)	Explanation
Slower rebuild				
High	High	Overexploited	−10	Watch and wait
High	Stable	Underexploited	+10	SPR high under stable catches
High	Low	Underexploited	+10	Possibly restrictive management
Stable	High	Overexploited	−10	SPR stable, but fishing is increasing
Stable	Stable	Fully exploited	0	SPR stable around reference
Stable	Low	Low exploitation	+10	Possibly restrictive management
Low	High	Depleted	−20	Recruitment overfishing possible
Low	Stable	Depleted	−10	Recruitment overfishing possible
Low	Low	Depleted	0	Recruitment overfishing possible
Extremely low	High	Very depleted	−20	Rebuild abundance
Extremely low	Stable	Very depleted	−10	Rebuild abundance
Extremely low	Low	Very depleted	−10	Rebuild abundance
Faster rebuild				
High	High	Overexploited	−10	Watch and wait
High	Stable	Underexploited	+10	SPR high under stable catches
High	Low	Underexploited	+10	Possibly restrictive management
Stable	High	Overexploited	−10	SPR stable, but fishing is increasing
Stable	Stable	Fully exploited	0	SPR stable around reference
Stable	Low	Low exploitation	+10	Possibly restrictive management
Low	High	Depleted	−20	Recruitment overfishing possible
Low	Stable	Depleted	−10	Recruitment overfishing possible
Low	Low	Depleted	0	Recruitment overfishing possible
Extremely low	High	Very depleted	−20	Rebuild abundance
Extremely low	Stable	Very depleted	−20	Rebuild abundance
Extremely low	Low	Very depleted	−20	Rebuild abundance

Notes: Two decision trees are described that differ with respect to rebuilding red abalone abundance. The harvest rate ratio U/U_{MSY} indicated whether catches were considered high (i.e., U/U_{MSY} was >1.0), low (i.e., U/U_{MSY} was <0.75), or stable ($0.75 \leq U/U_{MSY} \leq 1.0$). The SPR ratio SPR/SPR_{MSY} indicated whether site status was high ($SPR/SPR_{MSY} > 1.1$), stable ($0.9 < SPR/SPR_{MSY} \leq 1.1$), low ($0.5 < SPR/SPR_{MSY} \leq 0.9$), or extremely low ($SPR/SPR_{MSY} \leq 0.5$).

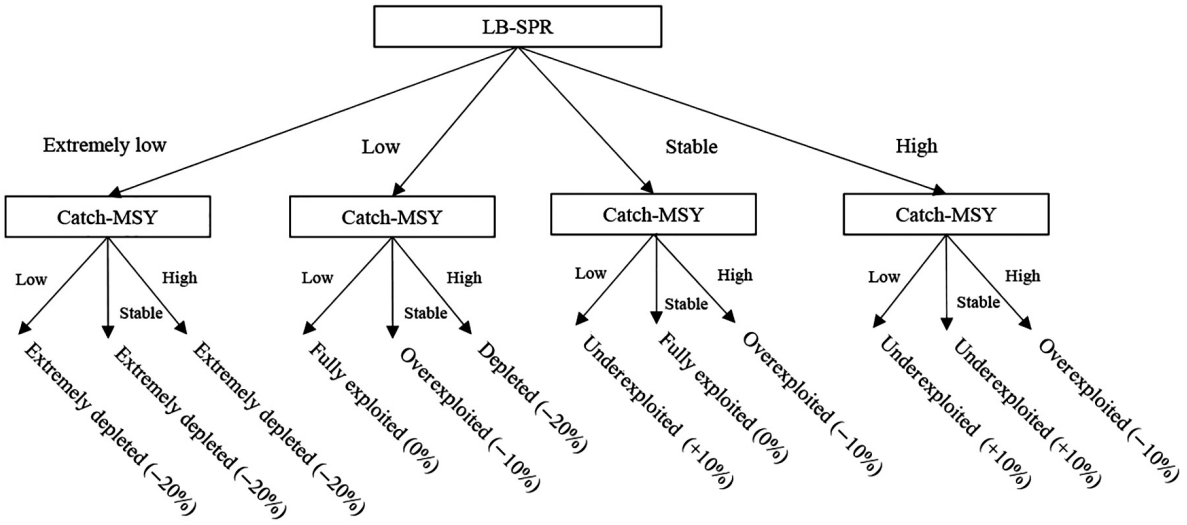

Fig. 2. Faster rebuild variant of the red abalone decision tree.

Table 4. Breakout rules in instances where length frequency data or catch time series are not available or are not included in the analysis.

Indicator	TAC adjustment (%)
Catch history	
High	−10
Stable	0
Low	+10
Length frequency data (for either fast and slow rebuilding)	
High	+10
Stable	0
Low	−10
Extremely low	−20

management experience with other abalone species (Prince 2005, Prince et al. 2008). In instances where one data stream became unavailable, breakout rules were specified to cope with the remaining indicator (Table 4).

It is worth noting how our chosen status indicators function cohesively. Catch histories are available for nearly all sites (no-take MPAs are excluded for obvious reasons) and were used to estimate the current harvest ratio for each site. But this indicator only reflects current harvest intensity and does not reveal whether the cumulative effects of past harvesting and environmental conditions have rendered the stock in a state where recruitment overfishing is likely to be occurring. The SPR ratio provides an indication of recruitment overfishing (Mace and Sissenwine 1993). When SPR levels trigger TAC reductions because recruitment overfishing is occurring, the harvest rate ratio works as a mitigating factor that recognizes when harvesting has been sufficiently reduced to theoretically induce stock rebuilding. Thus, since rebuilding is a slow process, the harvest rate ratio prevents ad nauseam TAC reductions (while SPR is low) and instead recognizes when reductions should be sufficient for rebuilding. Additionally, our chosen SPR and fishery exploitation indicators work non-antagonistically because they both work, more or less, to guide the stock to a biomass level associated with production of MSY.

Catch-MSY is a numerical routine that identifies plausible combinations of intrinsic rate of increase r and unfished vulnerable stock size B_0, given the site-specific input of a catch history. The estimation routine proceeds by drawing samples from specified prior distributions for r and B_0. Using the Schaefer surplus production model, reconstructed stock size trends are compared against plausible benchmarks for depletion in the initial year and final year of the time series. Parameter combinations of r and B_0 that satisfy plausibility criteria about stock depletion are retained. Plausible parameter ranges for depletion in the initial year and final year were specified following the procedure outlined in Martell

and Froese (2012). The initial depletion range was 0.5–0.9 when the catch in the initial year was less than half of the maximum annual catch; otherwise, the initial depletion range was 0.3–0.6. The final year's depletion was 0.3–0.7 when the catch in the final year was greater than half of the maximum annual catch; otherwise, the final year's depletion range was 0.01–0.4. These quantities were calculated separately for each site and re-calculated annually as part of each iterative application of the management strategy. Retained r and B_0 combinations were used to estimate the median value of the ratio U/U_{MSY}, where $U_{MSY} = r/2$ and current U is the catch in the final year divided by B_0 times median depletion. Given that red abalone catches were available for 56 sites, we leveraged information across sites to develop an informative prior for r, which occurred in two steps. First, 100,000 draws of r from a diffuse prior (Uniform[0.05, 0.15]) were made and identically applied to each site. Second, the subset of those 100,000 draws that satisfied the plausibility criteria for at least 25% of sites were retained, and the remaining r values were discarded. The retained r values were used as an informative prior and re-applied to each site, producing final estimates of U/U_{MSY}. This approach gleans information about r from sites where catch histories are informative about this quantity, and then leverages this information to produce derived quantities for each site. Throughout, priors for B_0 were diffuse, delineated using the default approach from Martell and Froese (2012), and independently specified for each site to reflect site-specific scaling. At each site, the estimated harvest rate ratio was used to indicate whether catches were considered high (i.e., U/U_{MSY} was >1.0), low (i.e., U/U_{MSY} was <0.75), or stable ($0.75 \leq U/U_{MSY} \leq 1.0$).

The theoretical basis for the LB-SPR method is that total mortality (Z) will affect the length frequency distribution of the stock and accordingly affect SPR. Thus, sampling of length frequency distributions can be used to infer current SPR, given a few additional life history parameters (Hordyk et al. 2015*b*). The maximum-likelihood LB-SPR estimation routine requires input parameters of M/K, asymptotic length, coefficient of variation of asymptotic length, and a logistic maturity curve (Hordyk et al. 2015*c*). For all sites, M/K was specified as 0.9, which conformed to M and K expectations for abalone life history (Prince et al. 2015). We specified the default coefficient of variation of asymptotic length to be 0.1 but allowed this parameter to increase up to 0.3 in instances where statistical convergence could not be obtained using the default value. Because emergence is thought to reflect site-specific maturation trends (e.g., Prince et al. 1988), logistic maturity parameters ($L50$ and $L95$) were obtained from the emergence trends captured in the left-hand side of the length frequency distribution (see Appendix S1). By identifying cumulative emergence probability-at-length using all length bins less than or equal to the mode of the length frequency distribution, we were also able to delineate the corresponding length at 50% maturity (e.g., $L50$). Having site-specific $L50$ was useful so that spatial variability in growth could be reflected in the LB-SPR fitting routine. From the $L50$ estimate, we calculated site-specific asymptotic length according to the ratio $L50/L\infty = 0.48$ and the length at 95% maturity according to the ratio $L95/L50 = 1.15$ (both ratios are based on empirical analysis of red abalone data; see Appendix S1).

Because length frequency data were only collected at several sites of the 56 sites in any given year, any site where length frequency sampling occurred within the previous three years was utilized in calculating the current site-specific SPR. If a site was sampled more than once during the previous three years, the most recent sampling event was used. The site-specific length-based indicator was the ratio of current SPR to the SPR expected to produce MSY in the long term. The quantity SPR_{MSY} was uniquely obtained for each of the sampled sites, as inter-site life history differences often do not support the use of a regional assumption about SPR that will ensure optimal recruitment (Shepherd and Baker 1998). Site-specific SPR_{MSY} was calculated using a numerical routine in the LB-SPR library in R, in which equilibrium stock conditions (i.e., SPR and relative catches) are calculated for each incremental value in a series of fishing mortality rates (Hordyk et al. 2016). These calculations use the identical set of parameter inputs and equations used in site-specific SPR estimation, plus specification of steepness at 0.6, and enable SPR_{MSY} to be identified. For sites where monitoring did not occur, the median of site-specific SPR ratios was

taken separately for each of two regions (Sonoma County and southward or Mendocino County and northward). At each site, the median SPR ratio or the site-specific SPR ratio (whichever was available) was used to determine indicator status of high ($SPR/SPR_{MSY} > 1.1$), stable ($0.9 < SPR/SPR_{MSY} \leq 1.1$), low ($0.5 < SPR/SPR_{MSY} \leq 0.9$), or extremely low ($SPR/SPR_{MSY} \leq 0.5$).

Spatial allocation of fishing and regional regulatory adjustments

Given the practical challenges associated with utilizing site-specific TACs for a regional fishery with widespread interest from fishers, two regional TACs were implemented. Using the Sonoma–Mendocino county line, one region consisted of Mendocino and northward (i.e., Mendocino, Humboldt, and Del Norte counties) and the other consisted of Sonoma and southward (i.e., Sonoma and Marin counties). Depending on practicality, monitoring, and enforcement capabilities, regions can be further broken into smaller sizes, if desired. Using the decision tree, site-specific TAC adjustments were made. These site-specific TACs were then summed across sites within a region to produce the regional TAC. In applying this approach, TAC adjustments to sites with the largest catches will have the greatest effect, or weighting, on the regional TAC. Thus, changes to the entire coastline are most predominantly affected by fishing sites with the highest catches, which also tend to be sites that are subject to length frequency monitoring and are believed to be experiencing the highest relative levels of exploitation.

Regional TACs were removed (harvested) without error; however, implementation error occurred at the level of site-specific removals. We utilized a spatial effort allocation model that increased or decreased regional effort as necessary to achieve removal of the regional TAC, while maintaining the relative spatial distribution of effort commensurate with the simulated 2016 effort distribution. This effort allocation model reflected the idea that each site would continue to maintain its relative popularity with fishers into the foreseeable future, despite local abundance changes. Consequently, site-level implementation error was an emergent property of the simulations, not a pre-specified level of precision. In initial model development, we also considered alternative effort allocation models; however, resulting simulation results did not vary dramatically between model formulations, and thus, we opted to utilize only a single effort allocation framework (Harford et al. 2017).

Baseline performance testing

Management strategies were examined against a factorial combination of operating models reflecting two historical abundance scenarios and two forecasting scenarios about future environmental conditions. To construct these operating model combinations, model tuning was carried out using the actual datasets and their corresponding indicator quantities for the time period of 2002–2016 (Appendix S2). Uncertainty associated with reconstructing historical conditions led us to consider two historical scenarios: Scenario 1: historical natural mortality baseline; and Scenario 2: historical natural mortality anomaly.

The baseline natural mortality scenario reflected visual tuning without recognition of possible natural mortality increases during the final years of the historical time period. Conversely, the second scenario considered concerns about high natural mortality during the final years of the historical time period (i.e., Rogers-Bennett et al. 2012) by including a 20% increase in natural mortality during the final 5 yr of the historical time period. This 20% natural mortality increase was arbitrary but was intended to reflect the possibility of recent anomalous losses of red abalone. In producing forecasts under different management strategies, two scenarios about environmental conditions involved simulating (1) future ENSO anomalies and (2) future ENSO anomalies plus severe episodic natural mortality fluctuations (i.e., harmful algal blooms) and episodic recruitment failures. Note that natural recruitment fluctuations (not to be conflated with recruitment failures) occurred during all historical and forecast scenarios. Collectively simulating historical scenarios, followed by forecast scenarios, reflected a variety of environmental conditions to which the red abalone are, at times, simultaneously subjected.

Management strategies were two variants of our decision tree, which differed principally in magnitude of TAC adjustment increments when the stock was thought to be at extremely low

sizes (Table 3). For comparison, a perfect-information reference HCR was also implemented. The reference HCR applied a constant fishing mortality rate of 0.048 yr^{-1}, which was the true simulated F_{MSY} as determined from equilibrium operating model characteristics. Forecasts of management strategies were conducted for 25-yr durations. All time- and space-varying stochastic parameter values were generated ahead of simulation runs and applied in parallel against each management strategy to ensure that all evaluations occurred against the same sequences of events, thus avoiding chance differences inherent in a sample of random draws from affecting performance outcomes (Punt et al. 2016). Consistent with current regulations, minimum harvest length of seven inches (178 mm) was used in all operating models, although we later explored this assumption in a sensitivity run in Appendix S3.

Four performance metrics were calculated using medians and measures of dispersion across 56 sites times 250 simulation runs. First, we measured spawning biomass by calculating the ratio of biomass in the 25th year of the forecasts to the biomass in first year of the forecasts. Second, we calculated the ratio of catches in weight in the 25th year of the forecasts to the catches in first year of the forecasts. Third, we calculated the ratio of biomass in the 25th year to B_{MSY}. Fourth, we calculated the ratio of catches in the 25th year to MSY in weight. These performance metrics were also calculated for the 10th year of the forecasts. We also parsed performance measure calculations according to sites with and without length frequency monitoring.

Probabilistic performance metrics were also measured. First, we calculated the probability that forecast biomass in the 25th year would be below $1/2B_{MSY}$ and the probability that forecast catches in weight in the 25th year would be below 1/2MSY. These metrics were calculated as the number of times in which a given event occurred for each site–simulation run combination divided by total site–simulation run combinations (e.g., 1000 counted events/(56 sites × 250 simulation runs) = 0.07). Second, we examined the time series between the first forecast year and the 25th year to calculate the propensity for the stock to be below $1/2B_{MSY}$ during any year of a 25-yr forecast. This metric was calculated as the fraction of site–simulation run combinations where biomass was below $1/2B_{MSY}$ for at least half of the 25-yr forecast duration. These metrics reveal the volatility associated with severe environmental conditions and the challenges faced in stock rebuilding under these conditions.

Rebuilding considerations

Given the fishery closure that occurred for the 2018 season, we aimed to provide general guidance on stock rebuilding using our two decision trees (Table 3). These two decision trees differed principally in the magnitude of TAC reductions imposed during extremely low stock sizes. For reference, we also report rebuilding trends associated with continued fishery closure and a constant catch policy proposed by a few interested fishers involving a constant TAC of 45,000 red abalone for the entire coastline, where the latter constant TAC was of interest to fishers. For comparison, preliminary reports of total catches for the fishery in 2015 and 2016 were 155,196 and 159,002, respectively. The constant TAC of 45,000 was divided between Mendocino region and Sonoma region in the ratio of 80–20%, reflecting the actual distribution of catches. For brevity, we initialized rebuilding following our historical time period of 2002–2016; thus, rebuilding begins in 2017 in our simulations.

Implementing annual bag limits

In this demonstration, we used annual bag limits to reflect a type of fishery control that is used for open-access fisheries. The decision tree variant named "faster rebuild" was modified for this task (Table 3). The decision tree was implemented in its original configuration, generating a regional TAC. Then, this regional TAC was compared against the previous year's regional TAC to identify the proportional change in target catch. Accordingly, the previous year's annual bag limit in a region was adjusted upward or downward using the corresponding proportional change in target catch, rounding down to the nearest integer. This decision tree was initialized using annual bag limits of 12 for Mendocino County and nine for Sonoma County, similar to actual regulations in 2016 and 2017. For simplicity, simulated fishers were constrained to fish in one of the two regions, where

in reality fishers can harvest red abalone from both regions if they are so inclined. We also imposed a lower annual bag limit of three to simulate a fishery that remained open even at low stock sizes. Given specification of the annual bag limit, the operating model requires this quantity to be translated into total removals. This was achieved by multiplying the annual bag limit times the number of fishers entering the fishery in a given year. Because entry to the fishery is independent of any other regulatory constraints (i.e., red abalone is open-access fishery), we specified three scenarios about future fishing effort. First, the number of fishers in 2016 (calculated based on removals and an assumed annual bag limits of 12 and 9 from Mendocino and Sonoma, respectively) was held constant during the simulated 25-yr time horizon. Second, we assumed effort would increase by 1% annually, which was slightly higher than the human population growth for the State of California in 2017 (and substantially higher than growth in Mendocino County, whereas Sonoma County experienced population decline; Anonymous 2018). Third, we assumed that effort would fluctuate in relation to the abundance of the entire red abalone stock (all 56 sites summed), which implies that higher abundance attracts fishers to the fishery, and vice versa, although the existence of such practices is not known for red abalone, using 2016 as a reference for red abalone abundance and related effort level adjustments.

Results

Baseline performance testing

Under typical ENSO-driven survival and growth patterns, our decision trees produced 25-yr forecasts with biomass tending to be at or above B_{MSY}, and with catches correspondingly below MSY (Fig. 3). Our results suggest that similar 25-yr performance of each respective management strategy occurred in the face of severe events, given baseline natural mortality (less-depleted) conditions at the outset of forecasts (compare Fig. 3A, C). Likewise, diminished performance is shared between scenarios with anomalous natural mortality increases (more-depleted) at the outset of forecasts, regardless of the specified scenario about environmental severity (compare Fig. 3B, D). As expected, comparing these two results highlights that stock status in 25 yr will differ depending on initial depletion levels, which is indicative of red abalone life history, but that robustness to environmental conditions is achievable. Tracking relative changes to stock biomass at 10- and 25-yr horizons illustrated increased biomass in the shorter term, with continued biomass maintenance over the longer term (Fig. 4). Catches tended to be diminished in the shorter term, facilitating biomass increases, but longer-term catches were similar to catch levels that existed at the outset of forecasts (Fig. 5).

Comparisons between sites that were subject to length-based sampling and those that were not sampled suggested that sampled sites had catches closer to MSY than did non-sampled sites, across all operating model scenarios (Table 5). Also, biomass levels at non-sampled sites tended to exceed those at sampled sites. The reason for this performance pattern is twofold. First, selection of sampling sites by Reef Check and CDFW tends to favor sites that have historically maintained the highest catches (Tables 1 and 2). These sites are also most likely to require large catch reductions. The corresponding regional TAC reductions affected non-sampled sites, reducing catches at these sites often more than was necessary, especially given that non-sampled sites generally experience less intense fishing pressure. When viewed from the perspective of the functioning of the entire management strategy, our results suggest that non-sampled sites are treated, perhaps inadvertently, in a precautionary manner that sacrifices optimal catches for increased biomass. Second, in conducting additional simulation testing, we found that in instances of erroneous estimates of the harvest rate ratio, errors tended to be made in the direction that led to cautionary catch levels. Catch-MSY enabled site-specific indicators for all sites; however, these simulations revealed that 41% of harvest rate ratios were correctly assigned to a catch-MSY indicator category, 39% were erroneously assigned to a higher exploitation rate category, and 21% were erroneously assigned to a lower category. This effect results in the infrequent achievement of MSY-level catches in exchange for more cautionary catch levels (Fig. 3).

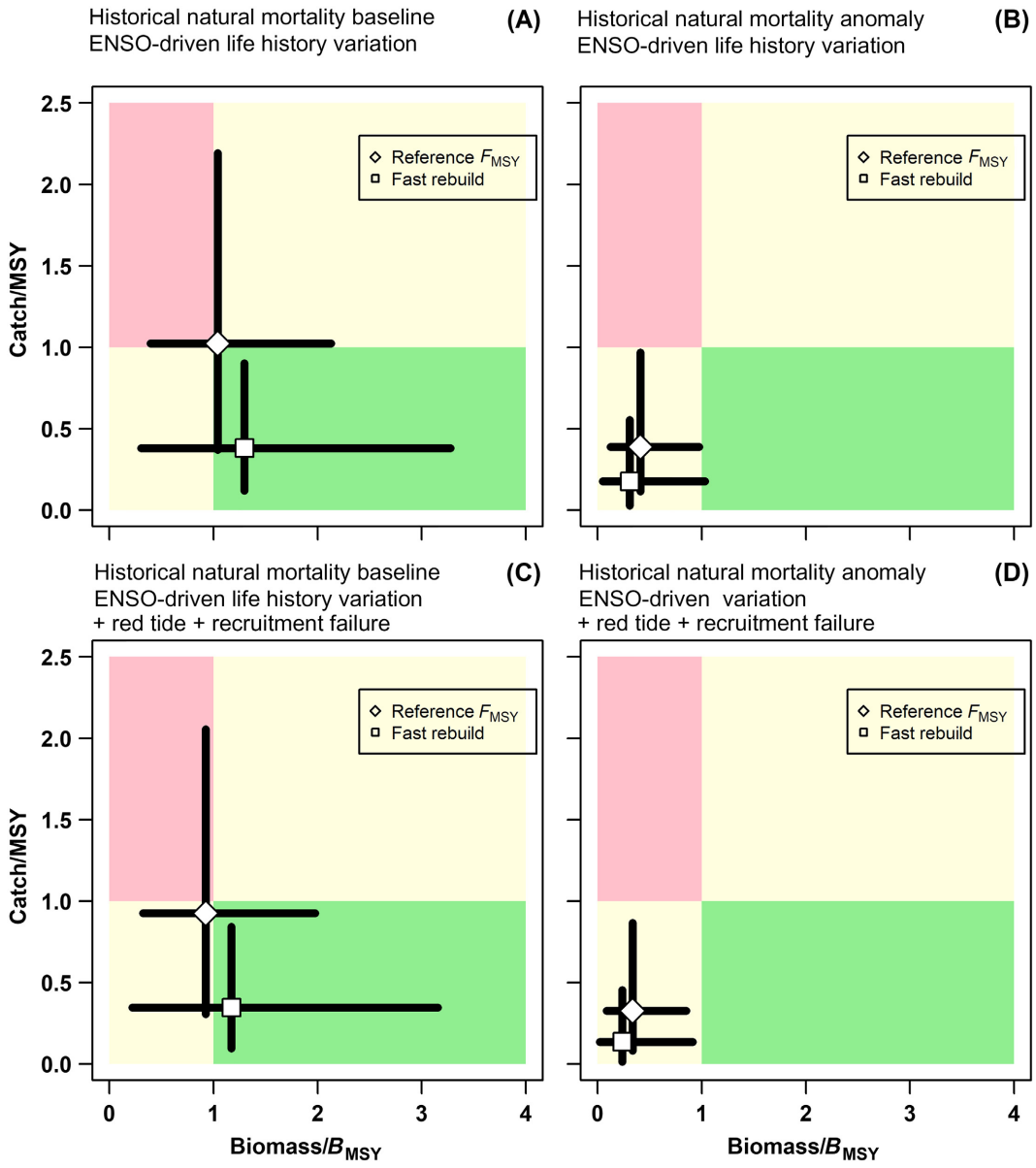

Fig. 3. Trade-off plots illustrating performance at the end of 25-yr forecasts for simulation scenarios (A, C) historical natural mortality baseline and (B, D) historical natural mortality anomaly. ENSO-driven life history variation was included in all plots, and severe natural mortality events and recruitment failure were included in C and D. The fast rebuild decision tree is contrasted against the reference F_{MSY} strategy. Slow rebuild is not shown, as very similar performance of decision trees occurred over this time horizon. Points are medians, and lines are centered 50% of simulation outcomes.

Rebuilding considerations

With fishery closure, rebuilding to B_{MSY} from the less-depleted stock condition at the outset of forecasts (i.e., baseline natural mortality scenario) had a median rebuilding time of 9 yr for both typical ENSO conditions and severe environmental conditions (Fig. 6). Both the faster rebuild and slower rebuild had similar median rebuilding times of 14 yr and 18 yr for the typical ENSO conditions and severe environmental conditions,

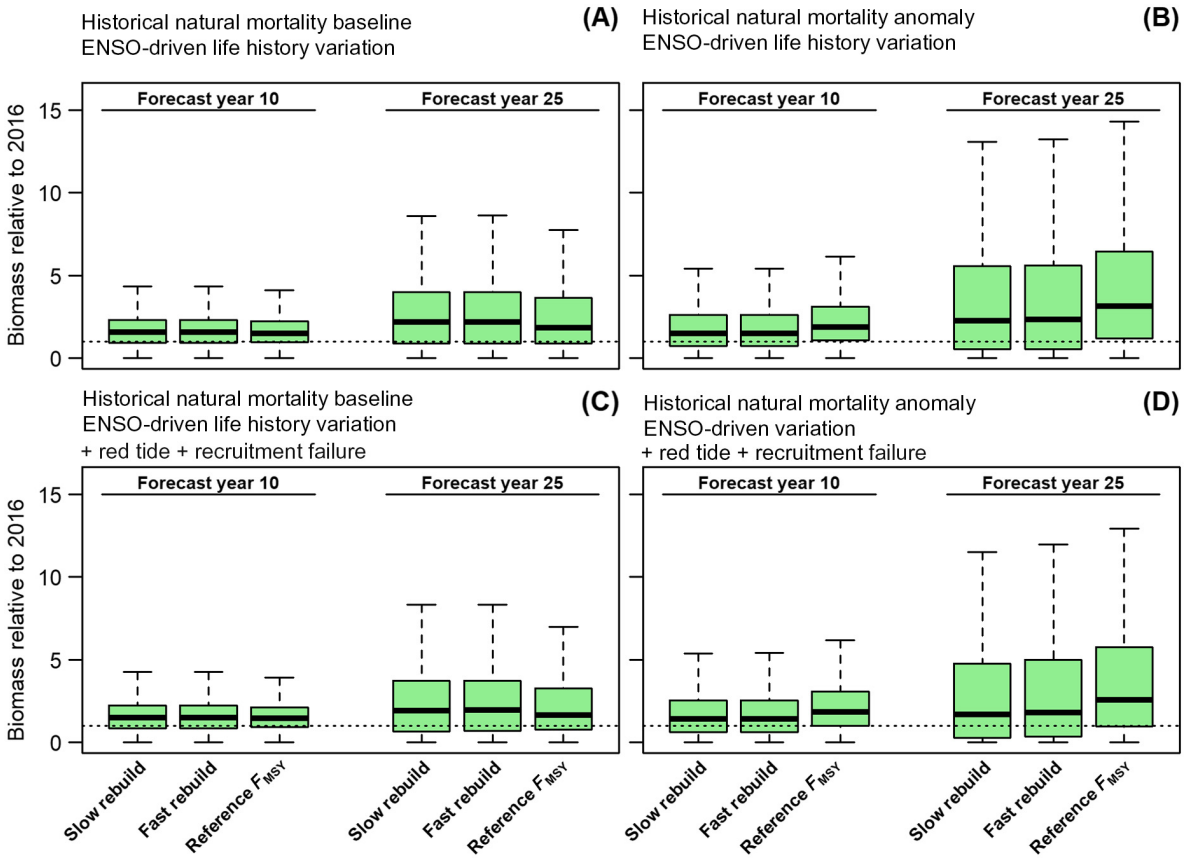

Fig. 4. Box plots of relative change in spawning biomass relative to initial year of forecasts for simulation scenarios (A, C) historical natural mortality baseline and (B, D) historical natural mortality anomaly. ENSO-driven life history variation was included in all plots, and severe natural mortality events and recruitment failure were included in C and D. Boxes show medians and interquartile ranges; whiskers are 1.5 times the interquartile range; horizontal dotted line at relative biomass of 1.0.

respectively. When the stock was substantially depleted at the outset of forecasts (i.e., historical natural mortality anomaly scenario), recovery time of faster rebuild and slower rebuild decision trees was considerably longer than the 25-yr time horizon that we simulated.

Probabilistic performance metrics were most useful in understanding stock trajectories under different conditions, and accordingly, in evaluating impediments to stock rebuilding (Tables 6–8). Shifting stock biomass from two different depleted states toward more productive state is a slow process for red abalone. Probabilities of sites having biomass below $1/2B_{MSY}$ after 25 yr of recovery tended to be >0.50, except under fishery closure, when rebuilding began from a more-depleted state (i.e., historical natural mortality anomaly scenario; Table 6). More optimistic rebuilding trajectories and potential for continued catches during rebuilding were evident given the baseline natural mortality scenario (less-depleted; Tables 6 and 7). By examining the entire time series and identifying instances where stock size fell below $1/2B_{MSY}$ during any year of a 25-yr forecast, we found notable differences in probabilities of such events between scenarios that differed in stock depletion at the outset of forecasts (Table 8). However, the simulated severity of environmental conditions was less detrimental to rebuilding trajectories than was the state of stock depletion at the outset of rebuilding. Thus, consistency in biological performance metrics regardless of the severity of environmental conditions reflects the ability of

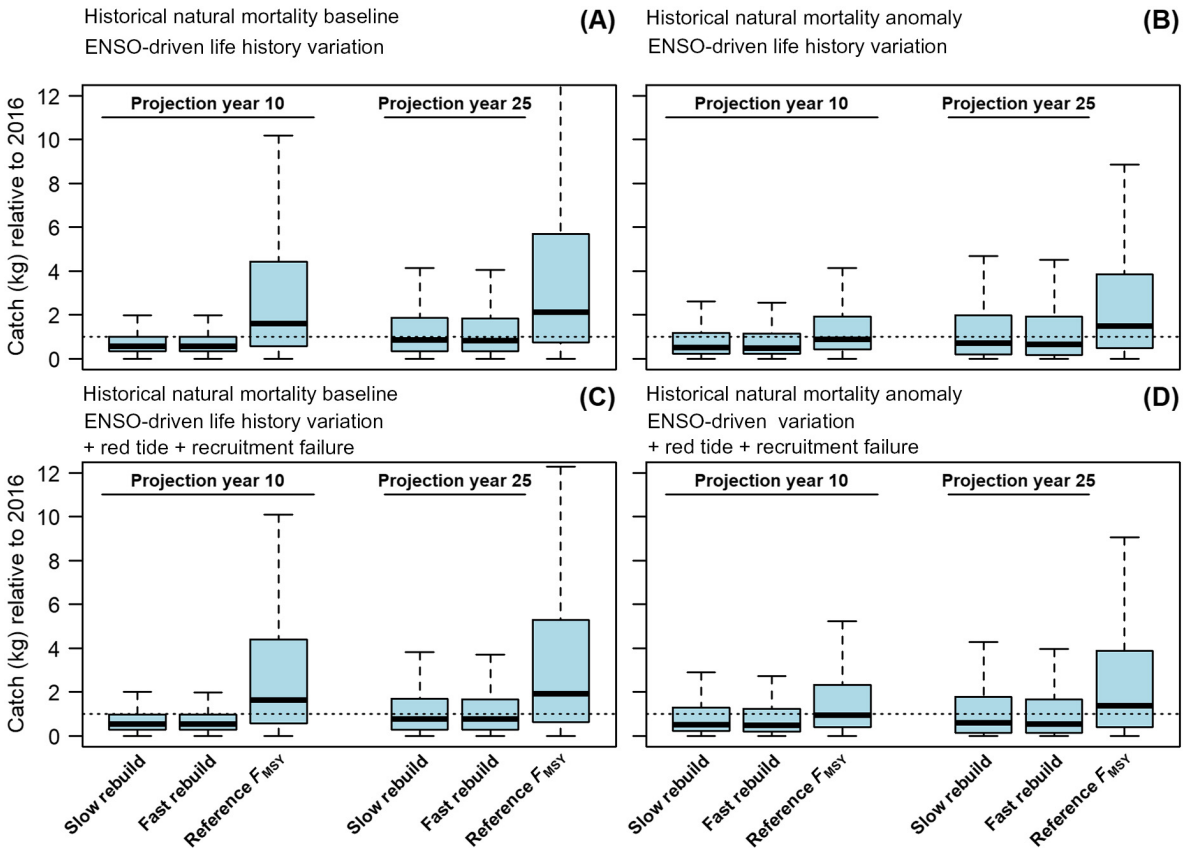

Fig. 5. Box plots of change in catches (weight) relative to initial year of forecasts for simulation scenarios (A, C) historical natural mortality baseline and (B, D) historical natural mortality anomaly. ENSO-driven life history variation was included in all plots, and severe natural mortality events and recruitment failure were included in C and D. Boxes show medians and interquartile ranges; whiskers are 1.5 times the interquartile range; horizontal dotted line at relative catches of 1.0.

the decision tree to reduce catches under severe conditions, as evidenced by reduced cumulative catches across 25-yr simulation runs during severe environmental events (Table 8). Consequently, biomass protection is maintained at the expense of catches, as environmental volatility necessitates.

Implementing annual bag limits

Our demonstration of annual bag limits highlights one approach to utilizing the decision trees in conjunction with regulatory tactics that are associated with recreational fisheries. Not surprisingly, MSY-based performance measures were consistent between management strategies implemented using annual bag limits or TACs (Fig. 7A). Since management strategy performance depended most strongly on depletion at the outset of forecasts, results are presented for two scenarios under ENSO-driven life history variation: historical natural mortality baseline and historical natural mortality anomaly (Fig. 7D, E). In plots that provide an example simulation run (one simulation out of 250 total runs using an annual bag limit and constant future fishery effort), two important characteristics of the decision tree are demonstrated (Fig. 7B, C). The first characteristic is that bag limits track stock abundance. The initially depleted state of the Mendocino region causes bag limit reductions, but as biomass rebounds slightly after 2025, bag limits increase, and importantly, bag limits stay below the initial 12 yr^{-1} as the biomass in the region has not

Table 5. MSY-based performance measures for 25-yr forecasts of two decision tree variants and a reference F_{MSY} rule.

Management strategy	Baseline natural mortality		Anomalous natural mortality	
	ENSO-driven variation	ENSO + episodic events	ENSO-driven variation	ENSO + episodic events
Performance metric: median B/B_{MSY}				
All sites (56)				
Slower rebuild	1.30 (2.81)	1.17 (2.81)	0.30 (1.24)	0.22 (1.28)
Faster rebuild	1.30 (2.81)	1.17 (2.81)	0.31 (1.24)	0.24 (1.29)
F_{MSY}	1.04 (1.54)	0.93 (1.50)	0.41 (0.87)	0.34 (0.86)
Sites with length sampling (15)				
Slower rebuild	1.20 (2.72)	1.06 (2.77)	0.27 (1.17)	0.19 (1.23)
Faster rebuild	1.20 (2.72)	1.07 (2.77)	0.27 (1.17)	0.20 (1.24)
Sites without length sampling (41)				
Slower rebuild	1.33 (2.84)	1.20 (2.82)	0.32 (1.26)	0.23 (1.30)
Faster rebuild	1.34 (2.84)	1.21 (2.82)	0.32 (1.27)	0.25 (1.31)
Performance metric: median *C*/MSY				
All sites (56)				
Slower rebuild	0.39 (1.02)	0.35 (0.96)	0.18 (0.86)	0.15 (0.78)
Faster rebuild	0.38 (1.01)	0.35 (0.95)	0.18 (0.85)	0.13 (0.74)
F_{MSY}	1.02 (1.71)	0.92 (1.68)	0.39 (0.96)	0.33 (0.96)
Sites with length sampling (15)				
Slower rebuild	0.48 (1.09)	0.44 (1.01)	0.22 (0.89)	0.19 (0.76)
Faster rebuild	0.47 (1.10)	0.43 (1.00)	0.21 (0.88)	0.17 (0.72)
Sites without length sampling (41)				
Slower rebuild	0.36 (0.99)	0.33 (0.94)	0.17 (0.84)	0.14 (0.78)
Faster rebuild	0.35 (0.99)	0.32 (0.92)	0.16 (0.83)	0.12 (0.75)

Notes: Column headings indicate operating model scenarios. *B* is spawning biomass and B_{MSY} is the spawning biomass that produces maximum sustainable yield, both in kg; *C* is catch and MSY is maximum sustainable yield, both in kg; ENSO is El Nino Southern Oscillation Index; episodic events include both increases in natural mortality and recruitment failures. Values in parentheses are SEs.

reached B_{MSY}. The second characteristic is that high biomass enables fishers to take advantage of favorable conditions. For the Sonoma region, an initial bag limit reduction is followed by rapid biomass recovery that surpasses B_{MSY}, and accordingly, bag limits continue to increase beyond the initial 9 yr^{-1}.

Discussion

Our management strategies were aimed at addressing five policy considerations for the red abalone fishery. First, site-specific indicators were desirable to inform decision-making, while also recognizing that guidance was needed for adjusting catches (or other management measures) at any spatial scale, including the entire coastline. Second, indicators needed to reflect the most reliable of existing data sources, rather than exploring alternative data streams. Third, flexibility needed to be maintained to accommodate additional monitoring sites, should monitoring programs expand (e.g., Freiwald et al. 2016). Fourth, flexibility needed to be maintained in HCR specification to accommodate tactical regulations associated with managing this open-access recreational fishery. Finally, HCRs needed to enable managers to implement regional regulations (perhaps using different spatial boundaries than we assumed herein).

We found that while decision tree performance was sensitive to depletion at the outset of forecasts, it was not sensitive to the environmental conditions that we simulated. In the face of severe environmental conditions, reasonable performance involving the protection of spawning biomass was achieved by reducing catches, as environmental perturbations necessitated. Management strategy robustness to environmental conditions is central to developing such approaches for red abalone because this species is particularly vulnerable to variability in

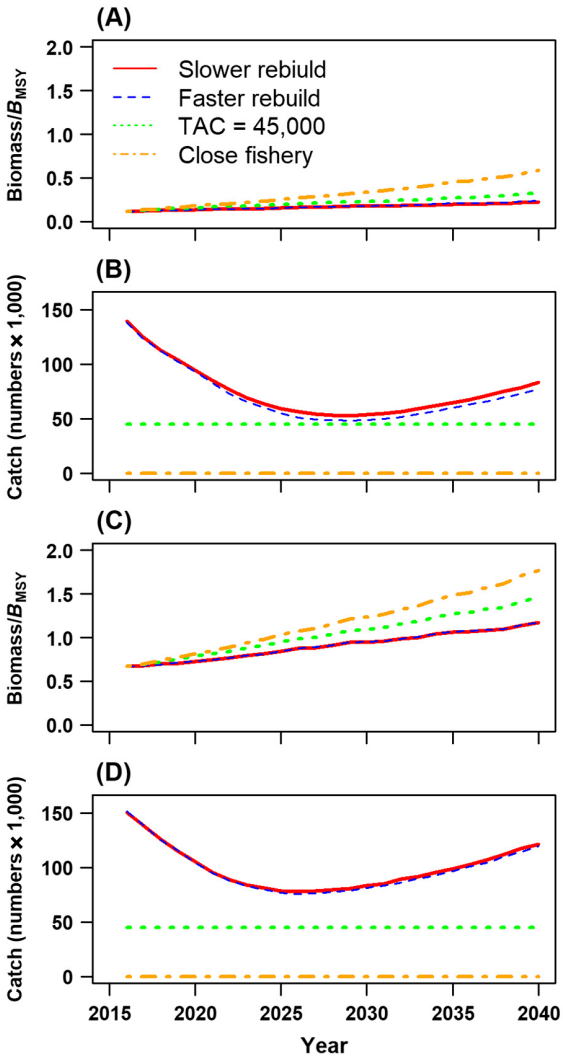

Fig. 6. Median rebuilding expectations under the severe environment scenario (i.e., ENSO-driven life history variation, severe natural mortality events, and recruitment failure). Shown are (A, B) simulation scenarios of historical natural mortality anomaly (more-depleted stock state) and (C, D) historical natural mortality baseline (less-depleted stock state). Median rebuilding expectations are presented in terms of (A, C) biomass relative to B_{MSY} and in terms of (B, D) total catches in numbers.

environmental conditions, which can affect survival, growth, and reproductive success (Tegner et al. 2001, Rogers-Bennett et al. 2012). Median rebuilding timeframes, when the simulated red abalone stock was highly depleted, exceeded the 25-yr time horizon of our forecasts. This result is concerning ecologically, particularly given the widespread need for rebuilding of California's abalone stocks, but this concern reflects the slow-growth biology of abalone species and similar concerns have been raised about other highly depleted abalone species (Catton et al. 2016).

The results of our MSE highlighted trade-offs that will require consideration by managers and stakeholders. First, our multi-indicator approach tended to maintain biomass levels that exceeded the biomass associated with maximum sustainable yield (B_{MSY}), but at a cost to catches, which remained less than MSY over the 25-yr time horizon. However, recent-past (2002–2016) catches were also unlikely to be at or near MSY, given our historical reconstructions (Appendix S2). Consequently, managers and stakeholders should consider whether recent-past catches were reasonable and whether forecasted catches, generated by the decision tree, would be considered similarly acceptable (compare Figs. 4 and 5). Second, the use of catch-MSY to calculate a harvest rate ratio enabled site-specific indicators for each site, but this indicator tended to err on the side of cautionary catch reductions in instances where estimated quantities were unreliable. Thus, the use of catch-MSY, in this instance, trades off the desirability of an indicator for each site, with lower catches than could be optimally obtained. Third, our candidate management strategies were conservative in terms of biomass protection at non-sampled sites. This is an example of the complex set of interactions that exist between components of a management strategy (i.e., site selection for surveys, data analysis, and HCR). The consequence of the spatial extent of length frequency sampling tended to result in lower catches at non-sampled sites (whether these catch reductions were needed or not), but consequently this approach improved protection of spawning biomass at non-sampled sites.

Given these trade-offs, we provide two suggestions for viewing our results cohesively and in a manner that could assist in selecting a management strategy. Selection practices sometimes involve deciding whether candidate management strategies satisfy minimum performance standards across a sufficiently broad set of conditions, or the least across the most severe of

Table 6. Probabilistic biomass performance for two decision tree variants.

Management strategy	Baseline natural mortality		Anomalous natural mortality	
	ENSO-driven variation	ENSO + episodic events	ENSO-driven variation	ENSO + episodic events
10th-yr performance metric: Pr [$B < 1/2B_{MSY}$]				
All sites (56)				
Slower rebuild	0.36	0.38	0.76	0.77
Faster rebuild	0.36	0.38	0.76	0.77
F_{MSY}	0.36	0.37	0.74	0.75
Close fishery	0.30	0.31	0.69	0.70
Constant TAC = 45,000	0.33	0.34	0.73	0.90
Sites with length sampling (15)				
Slower rebuild	0.38	0.39	0.77	0.77
Faster rebuild	0.38	0.39	0.77	0.77
Sites without length sampling (41)				
Slower rebuild	0.36	0.37	0.76	0.77
Faster rebuild	0.36	0.37	0.76	0.76
25th-yr performance metric: Pr [$B < 1/2B_{MSY}$]				
All sites (56)				
Slower rebuild	0.32	0.35	0.60	0.64
Faster rebuild	0.32	0.35	0.60	0.63
F_{MSY}	0.30	0.34	0.55	0.60
Close fishery	0.19	0.22	0.42	0.46
Constant TAC = 45,000	0.26	0.29	0.53	0.58
Sites with length sampling (15)				
Slower rebuild	0.34	0.36	0.61	0.66
Faster rebuild	0.34	0.36	0.61	0.65
Sites without length sampling (41)				
Slower rebuild	0.31	0.34	0.59	0.64
Faster rebuild	0.31	0.34	0.59	0.63

Notes: For reference, F_{MSY}, close-fishery, and constant TAC rules are reported, allowing rebuilding comparisons during the 10th year and 25th year. Column headings indicate operating model scenarios; B is spawning biomass and B_{MSY} is the spawning biomass that produces maximum sustainable yield, both in kg; Pr is probability; ENSO is El Nino Southern Oscillation Index; episodic events include both increases in natural mortality and recruitment failures.

plausible conditions. This decision-making procedure is known as satisficing (Miller and Shelton 2010). A related consideration, consistent with the precautionary approach, would require deciding whether candidate management strategies pose sufficiently low risk to the resource, including irreparable damage, across as many circumstances as possible (Darcy and Matlock 1999, Restrepo and Powers 1999).

In developing operating models, we needed to make a variety of assumptions about parameter values. Our operating models reflected current estimates of life history parameters (Rogers-Bennett et al. 2004, 2007, Kashiwada and Taniguchi 2007, Leaf et al. 2008), and we incorporated life history variation in space and time in a manner that was consistent with empirical and experimental evidence. Temporal variation in growth and survival were not simply stochastic independent variables but were together systematically linked to a shared environmental signal, resulting in simulation of co-varying growth and survival trends (Leaf et al. 2007, Jiao et al. 2010, Cavanaugh et al. 2011). We also simulated each site as a spatially explicit component of a larger red abalone stock, which is consistent with expectations related to larval dispersal, adult movement, and meta-population dynamics (Ault and Demartini 1987, Shepherd and Brown 1993, Gruenthal et al. 2007, Temby et al. 2007, Saunders et al. 2008, Coates et al. 2013). As a precaution against incidental reliance on larval exchange, which could inadvertently improve perception of management strategy performance, sites had no such exchange of red abalone recruits.

Sensitivity runs were carried out to examine ecological assumptions as well as those related to

Table 7. Probabilistic catch performance for two decision tree variants.

Management strategy	Baseline natural mortality		Anomalous natural mortality	
	ENSO-driven variation	ENSO + episodic events	ENSO-driven variation	ENSO + episodic events
10th-yr performance metric: Pr [C < 1/2MSY]				
All sites (56)				
Slower rebuild	0.74	0.75	0.87	0.87
Faster rebuild	0.74	0.75	0.87	0.87
F_{MSY}	0.36	0.37	0.74	0.73
Close fishery	1.00	1.00	1.00	1.00
Constant TAC = 45,000	0.88	0.88	0.89	0.90
Sites with length sampling (15)				
Slower rebuild	0.70	0.69	0.86	0.84
Faster rebuild	0.70	0.70	0.86	0.86
Sites without length sampling (41)				
Slower rebuild	0.75	0.77	0.87	0.87
Faster rebuild	0.75	0.77	0.88	0.88
25th-yr performance metric: Pr [C < 1/2MSY]				
All sites (56)				
Slower rebuild	0.57	0.59	0.72	0.75
Faster rebuild	0.58	0.60	0.73	0.77
F_{MSY}	0.31	0.34	0.57	0.60
Close fishery	1.00	1.00	1.00	1.00
Constant TAC = 45,000	0.85	0.85	0.85	0.86
Sites with length sampling (15)				
Slower rebuild	0.51	0.53	0.69	0.73
Faster rebuild	0.52	0.54	0.70	0.74
Sites without length sampling (41)				
Slower rebuild	0.59	0.61	0.73	0.76
Faster rebuild	0.60	0.62	0.74	0.78

Notes: For reference, F_{MSY}, close-fishery, and constant TAC rules are reported, allowing rebuilding comparisons during the 10th year and 25th year. Column headings indicate operating model scenarios; C is catch and MSY is maximum sustainable yield, both in kg; Pr is probability; ENSO is El Nino Southern Oscillation Index; episodic events include both increases in natural mortality and recruitment failures.

data inputs (Appendix S3). Given concern about the Allee effect on abalone stocks (Tegner et al. 1989, Shepherd and Brown 1993, Catton et al. 2016), sensitivity runs suggested that performance could be sensitive to this form of recruitment limitation when a threshold for this effect was specified to occur at depletion levels >0.05; however, the plausibility of various depletion levels, or associated abalone densities, as determinants of thresholds for recruitment limitation remains an unresolved question (Micheli et al. 2008). We also examined sensitivity to life history parameter inputs to the LB-SPR method. Given erroneous inputs of ±25%, positive bias in M/K ratio led to a negative effect on sustainable biomass, while negative bias in the $L50/L\infty$ ratio and positive bias in $L50$ both had negative effects on obtaining high catches, although, in each of these cases, variation in results was minor and was deemed not to be sensitive to these quantities as biomass remained, on average, above B_{MSY}. Sensitivity to consistent underreporting of catches across all years was also explored and performance was not sensitive to this reporting problem because we used a constant probability of underreporting and because we used a relative measure of harvest rate, obtained from the catch-MSY approach, and did not rely on an absolute metric like MSY. But as a precaution, this result does not suggest that the management strategy is robust to poaching; to the contrary, poaching itself is not controlled through an HCR and no viable HCR should be expected to prevent fishery collapse in the face of high poaching.

Our slower rebuild and faster rebuild scenarios were designed to achieve just that, different

Table 8. Probabilistic performance between the first forecast year and the 25th year.

Management strategy	Baseline natural mortality		Anomalous natural mortality	
	ENSO-driven variation	ENSO + episodic events	ENSO-driven variation	ENSO + episodic events
Pr [$B < 1/2B_{MSY}$]				
All sites (56)				
Slower rebuild	0.35	0.37	0.74	0.75
Faster rebuild	0.35	0.37	0.74	0.75
Close fishery	0.27	0.29	0.64	0.65
Constant TAC = 45,000	0.31	0.33	0.70	0.71
Median cumulative catches (no. red abalone)				
All sites (56)				
Slower rebuild	2,622,994	2,480,286	1,921,205	1,870,660
Faster rebuild	2,602,034	2,443,049	1,866,097	1,771,588
Constant TAC = 45,000	1,125,000	1,125,000	1,125,000	1,125,000

Notes: Probability of stock biomass being below $1/2B_{MSY}$ across the 25-yr durations was calculated as the fraction of site–simulation run combinations where biomass was below $1/2B_{MSY}$ for at least half of the time. For comparison, the median cumulative catches over 25-yr durations are shown. ENSO is El Nino Southern Oscillation Index; episodic events include both increases in natural mortality and recruitment failures.

rebuild trajectories. However, this was not the case for the operating model scenarios that we considered, as rebuilding trends were quite similar between the two decision trees (Table 8). In each of these decision trees, only two combinations of status indicators (i.e., branches of the tree) differed in their corresponding percent TAC change (Table 3). Accordingly, more pronounced TAC reductions are likely needed to enhance rebuilding time. It is worth noting that rebuilding plots also illustrate the relative responsiveness of the decision trees in making different magnitude TAC reductions under different levels of stock depletion. Magnitudes of TAC reductions differ in response to initial state of stock depletion (compare catch plots in Fig. 6A, B). Further, TACs tended to rebound faster when stock biomass was quickly rebuilt, while TACs rebounded more slowly when stock biomass also rebuilt slowly (compare catch plots in Fig. 6C, D), highlighting the functionality of the decision trees.

In formulating candidate management strategies for the red abalone fishery, our use of site-specific length frequency data offers some practical solutions to ongoing monitoring challenges. Obtaining measurements of site-specific indicators, especially given considerable variation in abundance between locations, is known to affect management success of abalone fisheries (McShane and Naylor 1995, Prince 2005, Prince et al. 2008, Geibel et al. 2010). Because diver-based observations of length frequency distributions can be expanded to accommodate additional sites, coverage of the coastline can be continually improved and new sites can be included in the decision tree as soon as they are added to monitoring programs. The SPR indicator that is estimated from length frequency data is compared to a biological reference point (i.e., an SPR reference point) that is independent of historical conditions that may be unknown. Arguably, reliance on length frequency data is also a means to addressing specific considerations of red abalone ecology. Length frequency distributions measure relative changes in size structure and are not dependent on the reliability of abalone counts (i.e., density surveys). Therefore, length frequency sampling appears to be less affected by depth-oriented movement or re-distribution of red abalone, as long as length sampling adequately covers the entire depth range of habitats and as along as post-exploitation sized individuals are not subject to size-based differences in detection probability. Lastly, there remains an unresolved complication pertaining to whether habitat conditions, including instances of low kelp density, affect detection probability or "catchability" during density surveys. Pronounced year-to-year changes in detection probability will affect the reliability of density estimates. When detection probability is affected by environmental conditions, the magnitude of bias in animal counts can co-vary with

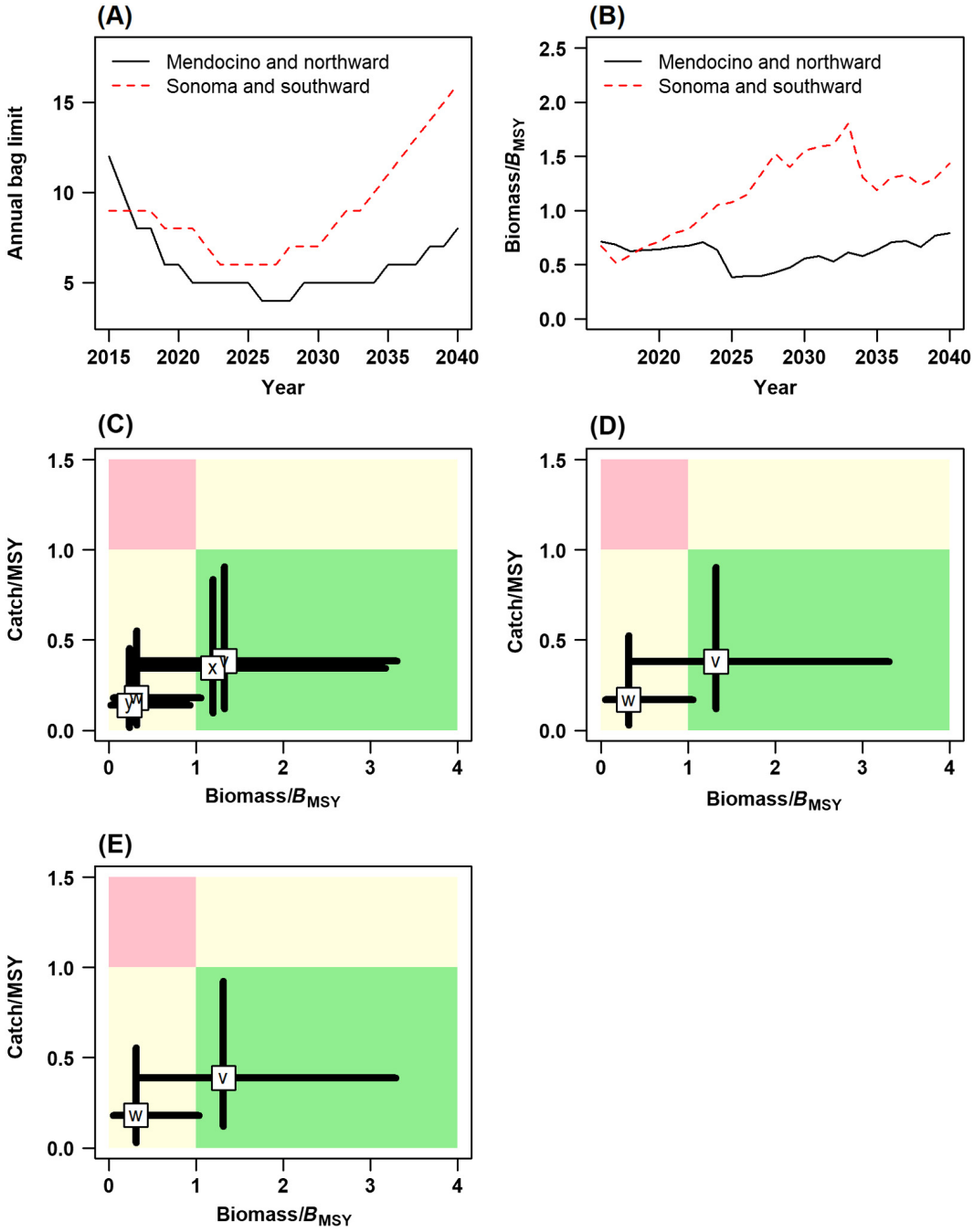

Fig. 7. Demonstration of the faster rebuilding decision tree that specifies adjustments to annual bag limits. (A) Example of one simulation run initialized at annual bag limits of 9 and 12 red abalone for Sonoma region and Mendocino region, respectively, and (B) corresponding regional biomass trends for the same simulation run. Scenarios are (C) constant entry to the fishery (effort), (D) entry to the fishery (effort) increasing by 1% annually, and (E) entry fluctuating in relation to red abalone abundance. Shown are performance metrics according to four operating model scenarios: v is historical natural mortality baseline, ENSO-driven life history variation; w is historical natural mortality anomaly, ENSO-driven life history variation; x is historical natural mortality baseline, ENSO-driven life history variation, red tide mortality, and recruitment failure; and y is historical natural mortality anomaly, ENSO-driven life history variation, red tide mortality, and recruitment failure.

environmental conditions (Royle and Dorazio 2009, Guillera-Arroita et al. 2010, Monk 2014).

Our evaluation of candidate management strategies necessarily reflected the data-limited state of the red abalone fishery. As it was applied here, MSE provided guidance on decision tree design, and in doing so, illustrated how pragmatism will be required in implementing an indicator-based approach. Pragmatism was reflected in our attempt to design a management strategy that reconciled capacity for achieving fishery objectives against practical impediments of data availability and data quality (Cadrin and Pastoors 2008, Dowling et al. 2015*b*, Harford et al. 2016). We also demonstrated that data-limited methods should be examined cautiously and be subjected to simulation testing. Data-limited approaches often rely on simplified models of complex stock dynamics, and if implemented without adequate evaluation, these approaches can sometimes result in poor management performance (Carruthers et al. 2014, Hordyk et al. 2015*a*, Fulton et al. 2016). Conversely, in some circumstances, performance of data-limited methods has been shown to be on a par with more complex approaches requiring the use of quantitative stock assessment (Geromont and Butterworth 2015). The application we have presented herein relates changes in indicator quantities to fish stock dynamics, and arguably, this type of approach has the potential to provide clarity to the process of developing fisheries policy and can lead to stakeholder buy-in (Campbell et al. 2007, Prince et al. 2008, Wilson et al. 2010).

Acknowledgments

We thank two anonymous reviewers for comments that led to the improvement of this manuscript. Funding for this study was provided by The Nature Conservancy. This research was carried out [in part] under the auspices of the Cooperative Institute for Marine and Atmospheric Studies (CIMAS), a Cooperative Institute of the University of Miami and the National Oceanic and Atmospheric Administration, cooperative agreement #NA10OAR4320143.

Literature Cited

A'mar, Z. T., A. E. Punt, and M. W. Dorn. 2010. Incorporating ecosystem forcing through predation into a management strategy evaluation for the Gulf of Alaska walleye pollock (*Theragra chalcogramma*) fishery. Fisheries Research 102:98–114.

Anderson, D. M., et al. 2008. Harmful algal blooms and eutrophication: examining linkages from selected coastal regions of the United States. Harmful Algae 8:39–53.

Anon. 2018. E-1 population estimates for cities, counties, and the state – January 1, 2017 and 2018. State of California, Department of Finance. http://dof.ca.gov/Forecasting/Demographics/Estimates/E-1/

Ault, J., and J. Demartini. 1987. Movement and dispersion of red abalone, *Haliotis rufescens*, in Northern California. California Fish and Game 73:196–213.

Bedford, R. A., J. W. Hearne, and H. K. Gorfine. 2013. Implications of the dichotomy between the spatial scales at which abalone are managed and harvested. Fisheries Management and Ecology 20:338–345.

Braje, T. J. 2016. Shellfish for the Celestial Empire: the rise and fall of commercial abalone fishing in California. University of Utah Press, Salt Lake City, Utah, USA.

Breen, P. A., S. W. Kim, and N. L. Andrew. 2003. A length-based Bayesian stock assessment model for the New Zealand abalone *Haliotis iris*. Marine and Freshwater Research 54:619–634.

Butterworth, D. S. 2007. Why a management procedure approach? Some positives and negatives. ICES Journal of Marine Science 64:613–617.

Butterworth, D. S., S. J. Johnston, and A. Brandão. 2010. Pretesting the likely efficacy of suggested management approaches to data-poor fisheries. Marine and Coastal Fisheries 2:131–145.

Butterworth, D. S., and A. E. Punt. 1999. Experiences in the evaluation and implementation of management procedures. ICES Journal of Marine Science 56:985–998.

Cadrin, S. X., and M. A. Pastoors. 2008. Precautionary harvest policies and the uncertainty paradox. Fisheries Research 94:367–372.

Campbell, R., C. Davies, J. D. Prince, D. Kolody, N. Dowling, M. Basson, P. Ward, K. McLoughlin, I. Freeman, and A. Bodsworth. 2007. Development and preliminary testing of the harvest strategy framework for the eastern and western tuna and billfish fisheries. Final Report to the Australian Fisheries Management Authority. CSIRO Marine and Atmospherics Research, Hobart, Tasmania, Australia.

Carruthers, T. R., A. E. Punt, C. J. Walters, A. MacCall, M. K. McAllister, E. J. Dick, and J. Cope. 2014. Evaluating methods for setting catch limits in data-limited fisheries. Fisheries Research 153:48–68.

Catton, C. A., K. L. Stierhoff, and L. Rogers-Bennett. 2016. Population status assessment and restoration

modeling of white abalone *Haliotis sorenseni* in California. Journal of Shellfish Research 35:593–599.

Cavanaugh, K., D. Siegel, D. Reed, and P. Dennison. 2011. Environmental controls of giant-kelp biomass in the Santa Barbara Channel, California. Marine Ecology Progress Series 429:1–17.

CDFW. 2005. Abalone recovery and management plan. Adopted by the California Fish and Game Commission. California Commission of Fish and Wildlife (CDFW), Monterey, California, USA.

Coates, J. H., K. A. Hovel, J. L. Butler, A. P. Klimley, and S. G. Morgan. 2013. Movement and home range of pink abalone *Haliotis corrugata*: implications for restoration and population recovery. Marine Ecology Progress Series 486:189–201.

Darcy, G. H., and G. C. Matlock. 1999. Application of the precautionary approach in the national standard guidelines for conservation and management of fisheries in the United States. ICES Journal of Marine Science 56:853–859.

Dowling, N. A., C. M. Dichmont, M. Haddon, D. C. Smith, A. D. M. Smith, and K. Sainsbury. 2015*a*. Guidelines for developing formal harvest strategies for data-poor species and fisheries. Fisheries Research 171:130–140.

Dowling, N. A., C. M. Dichmont, M. Haddon, D. C. Smith, A. D. M. Smith, and K. Sainsbury. 2015*b*. Empirical harvest strategies for data-poor fisheries: a review of the literature. Fisheries Research 171:141–153.

Emmett, B., and G. S. Jamieson. 1988. An experimental transplant of northern abalone, *Haliotis kamtschatkana*, in Barkley Sound, British Columbia. Fishery Bulletin 87:95–104.

Erlandson, J. M., T. C. Rick, M. Graham, J. Estes, T. Braje, and R. Vellanoweth. 2005. Sea otters, shellfish, and humans: 10,000 years of ecological interaction on San Miguel Island, California. Pages 58–69 *in* D. K. Garcelon and C. A. Schwimm, editors. Proceedings of the Sixth California Islands Symposium. Institute for Wildlife Studies and National Park Service, Arcata, California, USA.

Freiwald, J., A. Neumann, and D. Abbott. 2016. Red abalone size frequency survey protocol. Reef Check California, Reef Check Foundation, Marina del Rey, California, USA.

Froese, R., N. Demirel, G. Coro, K. M. Kleisner, and H. Winker. 2017. Estimating fisheries reference points from catch and resilience. Fish and Fisheries 18:506–526.

Fu, D. 2014. The 2013 stock assessment of paua (*Haliotis iris*) for PAU 3. New Zealand Fisheries Assessment Report 2014/44, Wellington, New Zealand.

Fulton, E. A., A. E. Punt, C. M. Dichmont, R. Gorton, M. Sporcic, N. Dowling, L. R. Little, M. Haddon, N. Klaer, and D. C. Smith. 2016. Developing risk equivalent data-rich and data-limited harvest strategies. Fisheries Research 183:574–587.

Geibel, J. J., J. D. DeMartini, P. L. Haaker, and K. Karpov. 2010. Growth of red abalone *Haliotis rufescens* (Swainson), along the north coast of California. Journal of Shellfish Research 29:441–448.

Geromont, H. F., and D. S. Butterworth. 2015. Complex assessments or simple management procedures for efficient fisheries management: a comparative study. ICES Journal of Marine Science 72:262–274.

Goodyear, C. P. 1993. Spawning stock biomass per recruit in fisheries management: foundations and current use. Page 120 *in* S. J. Smith and J. J. Hunt, editors. Risk evaluation and biological reference points for fisheries management. Special Publication in Fisheries and Aquatic Sciences, Ottawa, Canada.

Gorfine, H., B. Taylor, M. Cleland, M. Haddon, A. Punt, D. Worthington, and I. Montgomery. 2005. Development of a spatially-structured model for stock assessment and TAC decision analysis for Australian Abalone fisheries. Final report to Fisheries Research and Development Corporation Project No. 1999-116. Primary Industries Research Victoria, Queenscliff, Victoria, Australia.

Gruenthal, K. M., L. K. Acheson, and R. S. Burton. 2007. Genetic structure of natural populations of California red abalone (*Haliotis rufescens*) using multiple genetic markers. Marine Biology 152: 1237–1248.

Guillera-Arroita, G., M. S. Ridout, and B. J. T. Morgan. 2010. Design of occupancy studies with imperfect detection. Methods in Ecology and Evolution 1:131–139.

Haaker, P. L., D. O. Parker, and C. S. Y. Chun. 1995. Growth of black abalone, *Haliotis cracherodii* Leach, at San Miguel Island and Point Arguello, California. Journal of Shellfish Research 14:519–525.

Haddon, M. 2011. Modelling and quantitative methods in fisheries. Second edition. Chapman and Hall/CRC, New York, New York, USA.

Harford, W. J., N. A. Dowling, J. D. Prince, F. Hurd, L. Bellquist, J. Likins, and J. R. Wilson. 2017. Development of indicator-based harvest control rules for the northern California red abalone fishery. Prepared for the Nature Conservancy, Sacramento, California, USA.

Harford, W. J., T. Gedamke, E. A. Babcock, R. Carcamo, G. McDonald, and J. R. Wilson. 2016. Management strategy evaluation of a multi-indicator adaptive framework for data-limited fisheries management. Bulletin of Marine Science 92:423–445.

Hordyk, A. R., N. R. Loneragan, and J. D. Prince. 2015*a*. An evaluation of an iterative harvest strategy for data-poor fisheries using the length-based spawning potential ratio assessment methodology. Fisheries Research 171:20–32.

Hordyk, A. R., K. Ono, K. Sainsbury, N. Loneragan, and J. D. Prince. 2015*b*. Some explorations of the life history ratios to describe length composition, spawning-per-recruit, and the spawning potential ratio. ICES Journal of Marine Science 72:204–216.

Hordyk, A. R., K. Ono, S. Valencia, N. Loneragan, and J. D. Prince. 2015*c*. A novel length-based empirical estimation method of spawning potential ratio (SPR), and tests of its performance, for small-scale, data-poor fisheries. ICES Journal of Marine Science 72:217–231.

Hordyk, A. R., K. Ono, J. D. Prince, and C. J. Walters. 2016. A simple length-structured model based on life history ratios and incorporating size-dependent selectivity: application to spawning potential ratios for data-poor stocks. Canadian Journal of Fisheries and Aquatic Sciences 73:1787–1799.

Hulson, P.-J. F., D. H. Hanselman, and T. J. Quinn. 2012. Determining effective sample size in integrated age-structured assessment models. ICES Journal of Marine Science 69:281–292.

Jensen, A. L. 1996. Beverton and Holt life history invariants result from optimal trade-off of reproduction and survival. Canadian Journal of Fisheries and Aquatic Sciences 53:820–822.

Jiao, Y., L. Rogers-Bennett, I. Taniguchi, J. Butler, and P. Crone. 2010. Incorporating temporal variation in the growth of red abalone (*Haliotis rufescens*) using hierarchical Bayesian growth models. Canadian Journal of Fisheries and Aquatic Sciences 67:730–742.

Karpov, K. A., P. L. Haaker, D. Albin, I. K. Taniguchi, and D. Kushner. 1998. The red abalone, *Haliotis rufescens*, in California: importance of depth refuge to abalone management. Journal of Shellfish Research 17:863–870.

Kashiwada, J. V., and I. K. Taniguchi. 2007. Application of recent red abalone *Haliotis rufescens* surveys to management decisions outlined in the California abalone recovery and management plan. Journal of Shellfish Research 26:713–717.

Leaf, R. T., L. Rogers-Bennett, and P. L. Haaker. 2007. Spatial, temporal, and size-specific variation in mortality estimates of red abalone, *Haliotis rufescens*, from mark-recapture data in California. Fisheries Research 83:341–350.

Leaf, R. T., L. Rogers-Bennett, and Y. Jiao. 2008. Exploring the use of a size-based egg-per-recruit model for the red abalone fishery in California. North American Journal of Fisheries Management 28: 1638–1647.

Leighton, D. L. 2000. The biology and culture of the California abalones. Dorrance Publishing Company, Pittsburgh, Pennsylvania, USA.

Mace, P. M., and M. P. Sissenwine. 1993. How much spawning per recruit is enough? *In* S. J. Smith, J. J. Hunt, and D. Rivard, editors. Risk evaluation and biological reference points for fisheries management. Canadian Special Publication of Fisheries and Aquatic Sciences 120:101–118.

Martell, S., and R. Froese. 2012. A simple method for estimating MSY from catch and resilience. Fish and Fisheries 14:504–514.

Mayfield, S., C. Mundy, H. Gorfine, A. M. Hart, and D. Worthington. 2012. Fifty years of sustained production from the Australian abalone fisheries. Reviews in Fisheries Science 20:220–250.

McShane, P. E., K. P. Black, and M. G. Smith. 1988. Recruitment processes in *Haliotis rubra* (Mollusca: Gastropoda) and regional hydrodynamics in southeastern Australia imply localized dispersal of larvae. Journal of Experimental Marine Biology and Ecology 124:175–203.

McShane, P. E., and J. R. Naylor. 1995. Small-scale spatial variation in growth, size at maturity, and yield- and egg-per-recruit relations in the New Zealand abalone *Haliotis iris*. New Zealand Journal of Marine and Freshwater Research 29: 603–612.

Micheli, F., et al. 2008. Persistence of depleted abalones in marine reserves of central California. Biological Conservation 141:1078–1090.

Miller, D. C. M., and P. A. Shelton. 2010. "Satisficing" and trade-offs: evaluating rebuilding strategies for Greenland halibut off the east coast of Canada. ICES Journal of Marine Science 67:1896–1902.

Monk, J. 2014. How long should we ignore imperfect detection of species in the marine environment when modelling their distribution? Fish and Fisheries 15:352–358.

Moore, J. D., B. C. Marshman, and C. S. Y. Chun. 2011. Health and survival of red abalone *Haliotis rufescens* from San Miguel Island, California, USA, in a laboratory simulation of La Niña and El Niño conditions. Journal of Aquatic Animal Health 23:78–84.

Nash, W. J. 1992. An evaluation of egg-per-recruit analysis as a means of assessing size limits for blacklip abalone (*Haliotis rubra*) in Tasmania. Pages 318–338 *in* S. A. Shepherd, M. J. Tegner, and S. A. Guzmán del Proo, editors. Abalone of the world: biology, fisheries and culture. Blackwell, Oxford, UK.

NOAA. 2017. National Weather Service, Climate Prediction Center. Ocean Nino Index 3 month running means. http://www.cpc.ncep.noaa.gov/products/analysis_monitoring/ensostuff/ensoyears.shtml

OST. 2014. Scientific and technical review of the survey design and methods used by the California Department of Fish and Wildlife to estimate red abalone (*Haliotis rufescens*) density. California Ocean Science Trust (OST), Science Advisory Committee, Oakland, California, USA.

Perez, E. P. 2010. Una modificación de la ecuación de crecimiento de von Bertalanffy para incluir el efecto de la temperatura en el crecimiento del abalón rojo *Haliotis rufescens* para su uso en acuicultura. Revista de Biología Marina y Oceanografía 45:303–310.

Prince, J. 2005. Combating the tyranny of scale for haliotids: micro-management for microstocks. Bulletin of Marine Science 76:557–578.

Prince, J. D., A. Hordyk, S. R. Valencia, N. Loneragan, and K. Sainsbury. 2015. Revisiting the concept of Beverton-Holt life-history invariants with the aim of informing data-poor fisheries assessment. ICES Journal of Marine Science 72:194–203.

Prince, J. D., H. Peeters, H. Gorfine, and R. W. Day. 2008. The novel use of harvest policies and rapid visual assessment to manage spatially complex abalone resources (Genus Haliotis). Fisheries Research 94:330–338.

Prince, J. D., T. L. Sellers, W. B. Ford, and S. R. Talbot. 1987. Experimental evidence for limited dispersal of haliotid larvae (genus Haliotis; Mollusca: Gastropoda). Journal of Experimental Marine Biology and Ecology 106:243–263.

Prince, J. D., T. L. Sellers, W. B. Ford, and S. R. Talbot. 1988. Recruitment, growth, mortality and population structure in a southern Australian population of *Haliotis rubra* (Mollusca: Gastropoda). Marine Biology 100:75–82.

Punt, A. E., T. A'mar, N. A. Bond, D. S. Butterworth, C. L. de Moor, J. A. A. D. Oliveira, M. A. Haltuch, A. B. Hollowed, and C. Szuwalski. 2014. Fisheries management under climate and environmental uncertainty: control rules and performance simulation. ICES Journal of Marine Science: Journal du Conseil 71:2208–2220.

Punt, A. E., D. S. Butterworth, C. L. de Moor, J. A. A. De Oliveira, and M. Haddon. 2016. Management strategy evaluation: best practices. Fish and Fisheries 17:303–334.

R Development Core Team. 2012. R: a language and environment for statistical computing. R Development Core Team, Vienna, Austria.

Reid, J., L. Rogers-Bennett, F. Vasquez, M. Pace, C. A. Catton, J. V. Kashiwada, and I. K. Taniguchi. 2016. The economic value of the recreational red abalone fishery in northern California. California Fish and Game 102:119–130.

Restrepo, V. R., and J. E. Powers. 1999. Precautionary control rules in US fisheries management: specification and performance. ICES Journal of Marine Science 56:846–852.

Rogers-Bennett, L., B. L. Allen, and D. P. Rothaus. 2011. Status and habitat associations of the threatened northern abalone: importance of kelp and coralline algae. Aquatic Conservation: Marine and Freshwater Ecosystem 21:573–581.

Rogers-Bennett, L., R. F. Dondanville, C. A. Catton, C. I. Juhasz, T. Horii, and M. Hamaguchi. 2016. Tracking larval, newly settled, and juvenile red abalone (*Haliotis rufescens*) recruitment in Northern California. Journal of Shellfish Research 35:601–609.

Rogers-Bennett, L., R. F. Dondanville, and J. Kashiwada. 2004. Size specific fecundity of red abalone (*Haliotis rufescens*): Evidence for reproductive senescence? Journal of Shellfish Research 23:553–560.

Rogers-Bennett, L., R. Kudela, K. Nielsen, A. Paquin, C. O'Kelly, G. Langlois, D. Crane, and J. Moore. 2012. Dinoflagellate bloom coincides with marine invertebrate mortalities in northern California. Harmful Algae News 46:10–11.

Rogers-Bennett, L., D. W. Rogers, and S. A. Schultz. 2007. Modeling growth and mortality of red abalone (*Haliotis rufescens*) in northern California. Journal of Shellfish Research 26:719–727.

Rossetto, M., G. A. D. Leo, A. Greenley, L. Vazquez, A. Saenz-Arroyo, J. A. E. Montes, and F. Micheli. 2013. Reproductive potential can predict recruitment rates in abalone. Journal of Shellfish Research 32:161–169.

Royle, J. A., and R. M. Dorazio. 2009. Hierarchical modeling and inference in ecology. Elsevier, Boston, Massachusetts, USA.

Sainsbury, K., A. E. Punt, and A. D. M. Smith. 2000. Design of operational management strategies for achieving fishery ecosystem objectives. ICES Journal of Marine Science 57:731–741.

Saunders, T. M., S. Mayfield, and A. A. Hogg. 2008. A simple, cost-effective, morphometric marker for characterising abalone populations at multiple spatial scales. Marine and Freshwater Research 59:32–40.

Shepherd, S. A., and J. L. Baker. 1998. Biological reference points in an abalone (*Haliotis laevigata*) fishery. Pages 235–245 *in* G. S. Jamieson and A. Campbell, editors. Proceedings of the North Pacific Symposium on Invertebrate Stock Assessment and Management. Canadian Special Publication of Fisheries and Aquatic Science 125, Ottawa, Canada.

Shepherd, S. A., and L. D. Brown. 1993. What is an abalone stock: implications for the role of refugia in conservation. Canadian Journal of Fisheries and Aquatic Science 50:2001–2009.

Sloan, N. A., and P. A. Breen. 1988. Northern abalone, *Haliotis kamtschatkana*: fisheries and synopsis of life history information. Canadian Special Publication of Fisheries and Aquatic Science 103. NRC Research Press, Ottawa, Ontario, Canada.

Smith, A. D. M., K. J. Sainsbury, and R. A. Stevens. 1999. Implementing effective fisheries-management systems – management strategy evaluation and the Australian partnership approach. ICES Journal of Marine Science 56:967–979.

Tegner, M. J., P. A. Breen, and C. E. Lennert. 1989. Population biology of red abalones, *Haliotis rufescens*, in southern California and management of the red and pink, *H. corrugata*, abalone fisheries. Fishery Bulletin 87:313–339.

Tegner, M. J., and P. K. Dayton. 1987. El Nino effects on southern California kelp forest communities. Advances in Ecological Research 17:243–279.

Tegner, M. J., P. L. Haaker, K. L. Riser, and L. I. Vilchis. 2001. Climate variability, kelp forests, and the Southern California red abalone fishery. Journal of Shellfish Research 20:755–763.

Temby, N., K. J. Miller, and C. N. Mundy. 2007. Evidence of genetic subdivision among populations of blacklip abalone (*Haliotis rubra* Leach) in Tasmania. Marine and Freshwater Research 58:733–742.

Trainer, V. L., N. G. Adams, B. D. Bill, C. M. Stehr, J. C. Wekell, P. Moeller, M. Busman, and D. Woodruff. 2000. Domoic acid production near California coastal upwelling zones, June 1998. Limnology and Oceanography 45:1818–1833.

Vilchis, L. I., M. J. Tegner, J. D. Moore, C. S. Friedman, K. L. Riser, T. T. Robbins, and P. K. Dayton. 2005. Ocean warming effects on growth, reproduction, and survivorship of southern California abalone. Ecological Applications 15:469–480.

Watson, J., S. Mitarai, D. Siegel, J. Caselle, C. Dong, and J. McWilliams. 2010. Realized and potential larval connectivity in the southern California bight. Marine Ecology Progress Series 401:31–48.

Wilson, J. R., J. D. Prince, and H. S. Lenihan. 2010. A management strategy for sedentary nearshore species that uses marine protected areas as a reference. Marine and Coastal Fisheries 2:14–27.

Zhang, Z., A. Campbell, and J. Lessard. 2007. Modeling northern abalone, *Haliotis kamtschatkana*, population stock and recruitment in British Columbia. Journal of Shellfish Research 26:1099–1107.

Supporting Information

Additional Supporting Information may be found online at: http://onlinelibrary.wiley.com/doi/10.1002/ecs2.2533/full